2014-08-08

Modeling of Compositional Grading in Nonisothermal Reservoirs

Nikpoor, Mohammad Hossain

UNIVERSITY OF CALGARY

Modeling of Compositional Grading in Nonisothermal Petroleum Reservoirs

by

Mohammad Hossain Nikpoor

A THESIS

SUBMITTED TO THE FACULTY OF GRADUATE STUDIES

IN PARTIAL FULFILMENT OF THE REQUIREMENTS FOR THE

DEGREE OF MASTER OF SCIENCE

GRADUATE PROGRAM IN CHEMICAL AND PETROLEUM ENGINEERING

CALGARY, ALBERTA

JULY, 2014

Abstract

By far, in most reservoirs, even in most homogeneous ones, fluid properties are not the same all through the reservoir extent; the simplest reason is that the gravity makes a heavier fluid toward deeper zones. However, this is not always the case, because there are other reasons that may oppose this factor like a temperature gradient, capillary pressure, reservoir compartmentalization, reservoir filling, density overturn, and genesis processes. There are numerous reports of such phenomena in the literature.

This variation of composition can highly affect reserve estimation, production and EOR strategies and even a completion scheme (remember how a gas-oil ratio (GOR) and miscibility can change with depth as the fluid composition changes). As a result, more and more efforts have been devoted to including these effects in reservoir simulation through the initialization of a reservoir. Furthermore, some authors have tried to utilize this phenomenon to detect reservoir compartments. In this study, we consider the effects of gravity and thermal diffusion on the change of reservoir fluid composition and predict the location of possible GOC (gas-oil contact) in a reservoir. Additionally we develop a simple model to predict the change of the plus fraction molecular weight (MW) in a nonisothermal reservoir using continuous thermodynamics and the theory of irreversible processes. In two case studies, we validate our calculation procedure for the general compositional grading, GOC detection and the plus fraction MW change in the reservoir versus the data in the literature. The computational results show that the model developed works satisfactorily. Furthermore we will run several sensitivity analyses to show what factors affect the compositional grading modeling output and when the reservoir engineer should be concerned about severe change of fluid properties caused by compositional gradient.

UNIVERSITY OF CALGARY

FACULTY OF GRADUATE STUDIES

The undersigned certify that they have read, and recommend to the Faculty of Graduate Studies for acceptance, a thesis entitled "Modeling of Compositional Grading in Nonisothermal Reservoirs" submitted by Mohammad Hossain Nikpoor in partial fulfilment of the requirements of the degree of Master of Science.

Supervisor, Dr. Zhangxing (John) Chen, Department of Chemical and Petroleum Engineering

Dr. Jalal Abedi, Department of Chemical and Petroleum Engineering

Dr. Hassan Hassanzadeh, Department of Chemical and Petroleum Engineering

Dr. Behrouz Far, Department of Electrical and Computer Engineering

July 22, 2014

Date

Acknowledgements

The writing of a dissertation can be lonely and isolating experience, but yet it is obviously impossible without the personal and practical support of numerous people. Thus, my sincere gratitude goes to my supervisors Dr. Zhangxing (John) Chen at the University of Calgary for support and patience over the past years.

Table of Contents

List of Tables

List of Figures and Illustrations

List of Symbols, Abbreviations and Nomenclature

Symbol	Definition
BIP	Binary Interaction Coefficient
CCE	Constant Composition Expansion
CDF	Concentration Distribution Function
CG	Compositional Grading
EOS	Equation of State
GCE	Gravity-Chemical Equilibrium
GOC	Gas-Oil Contact
GOR	Gas-Oil Ratio
LGR	Liquid-Gas Ratio
MMC	Minimum Miscibility Concentration
MMP	Minimum Miscibility Pressure
MW	Molecular Mass
NHT	Net Heat of Transport
PR	Peng-Robinson Equation of State
PVT	Pressure-Volume-Temperature (Behavior)
Notations:	
1D	One Dimensional
3D	Three Dimensional
AMW	Concentration Distribution Function Parameter
BMW	Concentration Distribution Function Parameter
API	API gravity = 141.5/SPgr -131.5
Bo	Oil Formation Volume Factor
Bob	Oil Formation Volume Factor at the Bubble Point Pressure
c_k	Volume Correction Parameter of Component k
div	Divergence Operator
f_k	Fugacity of Component k
g	Gravitational Acceleration
H	Enthalpy
J_k	Mass Flux of Component k
J_q	Heat Flux
K_{ij}	Binary Interaction Coefficient
L_{ik}	Phenomenological Coefficient
M	Molecular Mass
P	Pressure
P_b	Bubble Point Pressure
P_c	Critical Pressure
Pd	Dew Point Pressure
Q^k_{net}	Net Heat of Transport of Component k

R	Universal Gas Constant
R_s	Solution Gas-Oil Ratio
S	Entropy
SPgr, S_g	Sg Specific Gravity
T	Temperature
T_b	Boiling Point Temperature
T_c	Critical temperature
T_R	Reservoir Temperature
U	Internal Energy
v_k	Partial Volume
$\overline{H}_i$	Partial Enthalpy
$\vec{V}$	Velocity Vector
$\Delta\overline{U}_i$	Partial Molar Internal Energy Departure
φ_k	Fugacity Coefficient of Component k
σ	Entropy Generation
μ	Chemical Potential (Partial Molar Gibb's Energy)
ρ	Density
η	Concentration Distribution Function Paramete

Chapter One: **Introduction**

1.1 Background

Petroleum has been the dominant source of energy for several decades and also one of the most important sources of raw material in the world. It has been of crucial interest to recover as much as possible from a reservoir without damaging it as it takes millions of years for the nature to produce the petroleum. This necessitates a good production strategy (primary, secondary or enhanced recovery) which itself calls for a proper understanding of petroleum composition within the reservoir.

As an example, in primary recovery, consider an oil reservoir with a high composition gradient. The fluid density and gas-oil ratio (GOR) vary with depth and we should decide where to perforate the wellbore casing in order to maximize the stock tank oil with lower gas production. In miscible gas injection, we should note that minimum miscibility pressure and concentration (MMP and MMC) are not the same at all depths as they are highly dependent on oil composition. The variation of fluid composition through the reservoir can greatly affect reserve estimation (Barrufet and Jaramillo, 2004) and production and EOR strategies (Riemens and Schulte, 1998; Syahrial, 1999; Hoier and Whitson, 2001; Luo and Barrufet, 2004; Jessen et al., 2008). It can also give important clues to detect reservoir compartmentalization (Smalley and England, 1992; Elshahawi et al., 2006) which highly affects economics of reservoir development and simulation studies. A relatively new but important aspect of the study is reservoir initialization (Salehirad, 2005). There are a lot more examples in the literature showing importance of the subject under study.

Numerous examples of petroleum reservoirs with significant compositional gradients (CG) can be found in the literature (Metcalfe et al., 1988; Hamoodi et al., 1994; de Oliveira Padua, 1997; Ghorayeb et al., 2000; Ratulowski et al., 2003; Hussein and Mahgoub, 2005; Gibson et al., 2006).

Most examples report decreasing methane content and solution gas-oil ratio and a decline in the amount of heptane and heavier components (C7+) with increasing depth. The variation of composition with depth generates a variation in other reservoir fluid properties, such as density, molecular weight, and saturation pressure. Compositional gradients are particularly important for thick reservoirs or reservoirs with a large structural relief. In extreme cases, CG may cause a stable liquid column over a lower density gas column in the reservoir (Ghorayeb et al., 2000) or even formation of a highly viscous hydrocarbon layer near the water-oil contact (Holt et al., 1983; Riemens and Schulte, 1988) which adversely undermines the recovery by water drive of an aquifer or water injection below the oil column to sweep oil towards production wells.

Several factors may lead to compositional variation within a reservoir, some of which are listed here:

1. Gravity (Sage and Lacey, 1939; Schulte, 1980; Whitson and Belery, 1994) causes heavier components to concentrate in deeper location and lighter ones in shallower location. The changes due to this effect are fairly small and linear with depth when the fluid condition is far away from the critical point and phase boundary of the petroleum fluid, and the effect becomes significant and nonlinear near the critical point and the phase boundary. The gravity effect is also called pressure diffusion in the literature (Ghorayeb and Firoozabadi, 2000c).
2. Thermal diffusion (Dougherty and Drickamer, 1955) causes a compositional gradient, both vertically and horizontally, when there is a temperature gradient in the reservoir vertically and horizontally, respectively. The usual behavior is an increase in the concentration of light components at location with higher temperature (Chaback and Lira-Galeana, 1992). Because a normal geothermal gradient causes the temperature to increase with depth, this

factor acts in the opposite direction of gravity in the vertical direction. It is normally weaker than the gravitational effect, and it causes a nonisothermal system to never reach equilibrium (a zero energy flux) even if a stationary (steady state) condition of a zero net mass flux is reached (Whitson and Belery, 1994). Thermal diffusion effects can be very strong near the critical points (as for most gas-condensate reservoirs) and cause highly nonlinear changes with depth and in an extreme case, a liquid can be stable on the top of vapor (Ghorayeb et al., 2000). Whitson and Belery (1994) mentioned that thermal diffusion can enhance, reduce or eliminate the gradient caused by gravity alone.

3. Incomplete hydrocarbon migration can cause a dynamic change of reservoir fluid composition with time and location in deposits. It has been observed that inflows of secondary fluid streams to the corners of the reservoir can cause a change in the fluid composition throughout the reservoir body (Gibson et al., 2006). These inflows usually have compositions totally different from the reservoir fluid compositions, severe lateral changes can be observed, and sometimes migration has been finished. However, as it takes 10's of millions of years for fluids to mix completely through reservoir extent, which may be 100 km in length, there has not been a complete mixing and one expects CG (Hoier and Whitson, 2001).
4. Natural convection (Ghorayeb and Firoozabadi, 2000) in gravitationally unstable systems may cause remarkable effects especially in high permeability or fractured reservoirs (Ghorayeb and Firoozabadi, 2000a). A weak convection can drastically change the composition both vertically and horizontally. Generally, convection is more rapid than diffusion (molecular, pressure, and thermal) because of nature of the processes involved (Smalley and England, 1992). Density overturn can cause fluid mixing vertically (Smalley

and England, 1992) while a horizontal convection affects laterally (Nasrabadi, 2006). A temperature gradient can cause thermally induced convection (Ghorayeb and Firoozabadi, 2000b; Jacqmin, 1990). Field-scale petroleum heterogeneities inherited from reservoir filling are unlikely to be homogenized by diffusion alone and require a more rapid process as convection (Smalley and England, 1992).

5. In some reservoirs, a dynamic flux of water from a partial aquifer (Hoier and Whitson, 2001) can serve as a sink for light components such as methane, and it can laterally and vertically change the reservoir fluid composition.
6. Asphaltene precipitation during migration can lead to different layers with different permeabilities to host different oil types (Sognesand, 1997), asphaltene is a part of the heavy-end molcules usually included in the plus fraction, when asphaltene precipitates, the remaining fluid will be lighter than the original fluid in place.
7. A sudden temperature change at the water-oil contact may cause asphaltene precipitation (Riemens et al., 1988; Hirschberg, 1988) which can result in the formation of a tar mat, and this layer of tar mat can limit the pressure maintenance by an aquifer for the reservoir and cause a lower primary recovery and failure of water injection projects.
8. Biodegradation (Temeng et al., 1998) has been reported in some reservoirs to produce hydrogen sulphide by a thermo-chemical reaction of sulphate and consuming the hydrocarbons as one group of reactants at elevated temperatures. It causes higher concentration of the acidic gas (and lower concentration of the hydrocarbon) at high-temperature zones (deeper location in the deposit).
9. Reservoir compartmentalization (Elshahawi et al., 2006) is one of the main concerns in petroleum reservoir development plans as a false description of the geological structure of

a deposit can result in a total economic failure of an oil field development plan. Sealing faults and shale breaks in a reservoir may cause limited pressure and fluid communication between different reservoir sections and highly affect the economic aspects of petroleum production from assets. Compartmentalization can be detected by compositional grading (CG) modeling studies with some care (Smalley et al., 1994), and it can cause step-like changes in composition of the reservoir fluid with location. Nevertheless, the geological and geophysical studies are the dominant tools. Sometimes, different source rocks filling different compartments of a reservoir result in reservoir sections with completely different fluids (Smalley et al., 1994).

10. Partial barriers cause limited fluid and pressure communication within hydrocarbon pool (Nasrabadi et al., 2008), high permeability sections of a layer separated by a very low permeability lamination, for example.
11. Genesis effects (Smalley and England, 1992) are related to source rocks. We may consider two situations: a) multiple source rocks feeding the reservoir and b) progressive maturation of a source rock; also, a combination of these two cases may occur.
12. Capillary forces (gas-oil interfacial curvature affected by a rock pore size) can oppose the gravity force in two-phase hydrocarbon reservoirs, which results in the formation of a transition zone from oil to gas instead of a sharp GOC (Lee, 1989; Wheaton, 1991); this effect is stronger at lower temperatures.
13. Artificial issues such as miscible gas injection into a specific point (wellbore in a reservoir) can cause oil in that part to become lighter than the points far from injection (Montel and Gouel, 1985), or production from a lower part of a naturally fractured reservoir may cause convection through fracture networks.

We cannot develop a model that takes into account all the aforementioned factors because of a lack of understanding of all the involved processes or facing very complex mathematical expressions with unknowns or changing boundary conditions. Most of the recent studies have considered the effect of gravity and thermal diffusion in a static fluid system where there is no flow in a reservoir (probably the condition encountered at the first day of exploration of a new reservoir when production has not begun) (Pedersen and Hjermstad, 2006; Nia and Movagharnejad, 2007). These studies use the gravitational-chemical-thermal diffusive force balance to describe the distribution of chemical compounds in the petroleum reservoir. In the case of two-phase petroleum reservoirs, some algorithms have been used to predict the location of GOC.

1.2 This Work

In this work, we develop the model to simulate variation in composition of a nonisothermal two-phase petroleum fluid column using an equation of state (EOS). We consider effects of gravity and temperature gradient with the assumption of stationary fluid (no net mass flux, steady state) and propose a new algorithm which is convenient to be used in the commercial reservoir simulators, and the algorithm can also predict the location of GOC in a two-phase hydrocarbon reservoir system. The model may not work for the cases where there is natural convetion or fluid flow caused by production in the reservoir.

Petroleum fluids consist of infinitely many components, and the usual practice is to report the mole fractions of several pure (or pseudo-) components, lump the remaining heavier part into one single pseudo-component, and call it as a plus fraction. It is obvious that this plus fraction will be a mixture of infinitely many components. Most of the time one considers the plus fraction as a pseudo-component with fixed physical properties in all the calculations involving an EOS but in

reality, the same factors leading to compositional variation in the reservoir can change the relative amounts of components within the plus fraction mixture. Therefore, the plus fraction MW and other properties change with respect to location in a reservoir. There are two works in the literature modeling this change, (Lira-Galeana et al., 1994; Nia and Movagharnejad, 2007). We assume the same two factors (gravity and thermal diffusion) with the same stationary assumption in developing the new model to predict the plus fraction MW change in the reservoir. We use continuous thermodynamics which treats the plus fraction as a mixture of infinitely many components described by a continuous concentration distribution function (CDF), and the same theory of irreversible processes used in the CG study to develop this model. At the same time, we also design a new strategy to model the sharp change in the plus fraction MW that is usually observed at GOC.

So, the problem to be solved is: given the composition, pressure, temperature, temperature gradient and the molecular weight of the plus fraction at depth h0, we seek the composition, pressure, and the molecular weight of the plus fraction at depth h.

In chapter 2 we will review the previous studies in the CG literature. In chapter 3 we will show a simple proof of the nonisothermal CG model used in this study and review the models proposed to nonisothermal term added to the isothermal model to account for the thermal diffusion term to convert the isothermal model into nonisothermal. In chapter 4 we derive our new model for the plus fraction MW with location in the reservoir and also propose a new and simple numerical algorithm to be used in the reservoir simulation initialization in order to calculate the composition, pressure and plus fraction MW in the reservoir extent. In chapter 5 we have validated our numerical algorithm for CG calculation and the plus fraction MW change with location in the reservoir with two sets of measured data from the literature and then run sensitivity analysis and study different

schemes of fluid distributions in two synthetic reservoirs. We summarize the findings in our work in the conclusions section.

Chapter Two: **Review of the Previous Works**

2.1 Theoretical Works in the Domain of Compositional Grading

In this section, we review some of the works within the domain of compositional grading. The elementary works considered only the effect of gravity (neglecting a temperature gradient) and assumed an isothermal reservoir. The formulation for calculating compositional variation under the force of gravity for an isothermal system was first given by Gibbs (1961) (so-called GCE, Gravity-Chemical Equilibrium model); his relationship is as follows:

$$\mu_i\left(P,Z,T\right)=\mu_i\left(P_{ref},Z_{ref},T\right)-M_i g\left(h-h_{ref}\right) \tag{2.1}$$

$$d\mu_i = RTdln\left(f_i\right) \tag{2.2}$$

$$f_i = f\left(EOS\right) \tag{2.3}$$

where P is the pressure, T the temperature, Z the fluid composition, M the molecular mass, μ the chemical potential, h the depth, *ref* shows the reference state, i the component index, R the universal gas constant, f the fugacity and g is the gravitational acceleration.

In 1930, Muskat addressed compositional variation with depth in petroleum reservoirs, and solved Eq. (2.1) for the simplified cases of (1) ideal solutions and (2) cases where all component molar volumes are equal. Two binary mixtures were treated in detail, and Muskat's oversimplified assumptions lead to the conclusion that compositional variations with depth due to gravity are negligible.

In 1938, Sage and Lacey came to the opposite conclusion when modeling composition with depth for a binary hydrocarbon liquid phase and a binary hydrocarbon gas (C_1−nC_4). They noticed that variations of GOR and specific gravity with depth had been observed in several hydrocarbon reservoirs. The authors found the compositional variations with depth to be significant in their

binary example. Calculations were based on solving Gibb's equation by assuming ideal solutions to evaluate the chemical potential, and using correlations to calculate partial volumes. Sage and Lacey made the important observation that the magnitude of the gravitational effect is large close to a critical point. Interestingly, they also commented that they suspected the effects estimated in the isothermal case would be *enhanced* if a temperature effect was included in the calculations.

From Sage and Lacey's important work until 1980 there have been several papers reporting reservoirs with compositional gradients. Schulte in 1980 extended the application of the isothermal gradient calculation by replacing the ideal solution behavior assumed in Sage and Lacey's work by a cubic EOS (Peng-Robinson or Soave-Redlich-Kwong). Schulte addressed the importance of using a valid EOS characterization by demonstrating the relatively large effect of binary interaction coefficients (BIPs) on the calculations. The author gave examples with saturated and undersaturated GOC in the Brent and the Statfjord formations of the Brent field, respectively, and observed that the saturation pressure gradient in the Brent Field was three to five times larger than that predicted by Schulte's approach.

A simplified formulation, including gravity and temperature separately was presented by Holt et al. in 1983. Example calculations, limited to binary systems, suggested that thermal effects can be of the same magnitude as gravity effects.

In 1988, Hirschberg discussed the influence of asphaltenes on compositional grading using a simplified two-component model (asphaltenes and non-asphaltenes). He showed that the asphaltene molecular weight strongly affects the calculated segregation, and this effect is more pronounced in lighter oils. He concluded that for oils with oil gravity less than 35° API, the compositional variations are mainly caused by asphalt segregation and the most important consequences are the large variations in oil viscosity and the possible formation of tar mats.

In 1985, Montel and Gouel presented an algorithm for solving the GCE problem using an incremental hydrostatic term instead of solving for pressure directly. The pressure does not follow the hydrostatic equation when there is temperature gradient within the reservoir. The geothermal gradient is always present in all petroleum reservoirs; the average temperature gradient within the earth's crust is 0.025 K/m which based on the Fourier's law of heat conduction, its value will be higher for less conductive formations.

Field case applications of GCE models were presented by Creek et al. in 1985 and Riemens and Schulte in 1988. They reported some difficulties in matching observed and calculated data but, at the end, it was shown that most compositional variations could be explained by the effect of gravity. Riemens and Schulte interpreted their case as a tar mat and reported an undersaturated gas-oil contact (GOC) in which both phases are present in the reservoir, but the reservoir pressure is over saturation pressure all through the reservoir thickness, which will be discussed in more details in this work.

Lee and Wheaton presented GCE models that included capillary forces in 1989 and 1991, respectively. Lee concluded that the effect of capillarity can become appreciable in the neighborhood of 1 μm pore radius. Wheaton concluded that neglecting CG effects can result in a 20% error in reserve calculations, and recommended mid-reservoir sampling to minimize errors.

In 1990, an attempt to combine the effects of gravity and a temperature gradient for a system of a zero net mass flux was presented by Belery and Silva. Their multicomponent model was an extension of an earlier work by Dougherty Jr. and Drickamer that was originally developed in 1955 for binary liquid systems. The comparison of calculated and observed data from the Ekofisk field in the North Sea is, however, not quantitatively accurate with or without a thermal effect.

An extensive discussion and a formal mathematical treatment of compositional grading using irreversible thermodynamics, including gravitational and thermal fields, was presented by Bedrikovetsky in 1993. Due to the lack of necessary information on the values of thermal diffusion coefficients, which in general are obtained experimentally only for certain mixtures in narrow ranges of pressure and temperature, only simplified models were proposed.

In 1994, Hamoodi and Abed presented a field case of a giant Middle East reservoir with areal and vertical variations in its composition. The reservoir in their study had horizontal temperature gradient which causes a gradient in the fluid composition in the horizontal direction.

A theoretical review of equilibrium formulation, including gravity and thermal diffusion was given by Faissat et al. in 1994. Unfortunately, no calculations were made to compare the different formulations. They presented the derivation for the following equation:

$$\nabla_T \mu_k = M_k g dh + M_k \left(Q^* - Q_k^*\right) \frac{\nabla T}{T} \qquad (2.4)$$

where the term $M_k \left(Q^* - Q_k^*\right)$ is called net heat of transport (NHT) and denoted by Q_k^{net}. We will deal with this term in the next chapter.

In 1996, Hamoodi et al. investigated some major mechanisms that affect the compositional variation, one being natural convection, based on a nonisothermal gravitational formulation for binary systems where the thermal diffusion terms are theoretically accounted for.

In 2000, Hoier and Whitson made a comprehensive evaluation of a simple model for vertical CG due to gravity, chemical and thermal effects with the simplifying assumption of a zero net component flux defining a "stationary" condition, and mentioned that this assumption may not be valid always as known in some fields. This assumption originates from these conditions: (1) no convection and (2) balance of driving forces, i.e., gravity, chemical and thermal.

Based on thermodynamics of irreversible processes, Ghorayeb and Firoozabadi (2000a, 2000b) and Firoozabadi et al. (2000) in three separate papers proposed theoretical expressions for modeling convection and diffusion of non-ideal and ideal multicomponent fluids in porous media, including an expression for thermal diffusion coefficients incorporating equilibrium properties, found from PR EOS, and non-equilibrium properties such as net heat of transport and energy of viscous flow, which is more reasonable than most of the previous models that used only equilibrium properties, as the process of thermal diffusion is a non-equilibrium one. They validated their model against published data, and their results showed a good match. Ghorayeb et al. (2000, April) used this model to interpret unusual fluid distribution in a Japanese field and got reasonable results comparing to the measured data. Their works have been the foundation to several theoretical and simulation works thereafter.

There is a large literature on molecular and thermal diffusion in the critical region for binary mixtures which was then extended to a multicomponent case; the works include experimental and modeling jobs done on a vast type of fluids (for a complete review of these models, refer to Nasrabadi's work in 2006).

During the current decade, a large number of works show applications of the previous models in reservoir characterization and other related subjects (Barrufet and Jaramillo, 2004; Luo and Barrufet, 2004; Salehirad, 2005; Pedersen and Lindeloff, 2003; Montel et al., 2003; Pedersen and Hjermstad, 2006). In 2008, Nasrabadi et al. presented a regular and comprehensive modeling of an unusual field case.

In many of the above models, a fixed molecular weight is assumed for the plus fraction, while the works by Lira-Galeana et al. (1994) and Nia and Movagharnejad (2007) showed that this is not the case. This new methodology, which is based on continuous and irreversible thermodynamics,

is able to predict variations of the plus fraction molecular weight in both isothermal and nonisothermal hydrocarbon reservoirs. If this change is large, one may have to split the plus fraction into a number of sub-fractions in order to minimize the error in reservoir simulation studies.

2.2 A Comparison between Equilibrium and Non-equilibrium Models

In equilibrium models, it is assumed that:

1. Temperature does not vary with depth.
2. Chemical equilibrium exists within a reservoir.
3. There is a zero mass flux in the reservoir (stationary state).
4. Mechanical equilibrium exists within the reservoir.
5. The only force acting on the reservoir fluids is the gravitational force.
6. There is no heat transfer in the reservoir.

Usually temperature increases with depth in the reservoir (the average geothermal gradient within the earth's crust is 0.025 K/m), so the first assumption is not true. Furthermore, the necessary condition for a thermodynamic equilibrium is an isothermal condition which is itself a bad assumption in many cases, so the second assumption is also incorrect. Moreover, we can reject the sixth assumption with the same reasoning. A Soret effect (a mass flux as a result of the temperature gradient) causes the fourth assumption also to be false. However, we sometimes compromise to get a simple model as we will see later in this study when we assume the heat flux to be zero in order to derive a model.

In the non-equilibrium model used in this study (1D modeling) we have assumed:

1. Temperature varies with depth.
2. There is no chemical equilibrium in the reservoir.

3. The mass flux of each component is zero (stationary assumption).
4. There is a heat flux in the system.
5. Mechanical equilibrium exists in the reservoir.
6. The only external force is the gravity.
7. Properties are assumed to be steady state (they do not change with time).
8. Deviation from the ideal (reversible) state is small enough to use the EOS.

So our model is superior to the isothermal model, but still approximate. To compare our model and the isothermal one, we should note that:

1. In most reservoirs, a concentration gradient calculated by an isothermal model is higher than that calculated by a nonisothermal one. This shows the contrasting effects of gravity and a temperature gradient.
2. In some reservoirs, an isothermal model is satisfactory in describing the fluid state.
3. A nonisothermal model predicts a composition gradient closer to the measured one. The isothermal model usually over-predicts it.
4. There are a few reservoirs with a composition gradient greater than that calculated by an isothermal model (one example is one with an unusual temperature gradient, in which the temperature gradient effect adds to the gravity effects instead of contrasting it (Ghorayeb et al., 2000, April).

In this thesis, we will model the compositional grading due to temperature variation and gravity using the stationary and no heat flux assumptions, the models may not be valid when there is convection in the reservoir.

2.3 Related Subjects

2.3.1 Undersaturated Gas-Oil Contact

In most cases, the concentration of heavy fractions decreases with elevation in the hydrocarbon column and as a result, the fluid critical temperature (T_c) decreases with elevation. An interesting situation occurs if the reservoir temperature (T or T_R) reaches this T_c (both T_c and T_R have a gradient; they may intersect each other at a point), and this will be a GOC (liquids are defined by $T<T_c$, while gases are defined by $T>T_c$). If at this point pressure is greater than the saturation pressure of the fluids, then the fluids will be undersaturated while both gas and liquid co-exist. Therefore, a so-called undersaturated GOC is present wherein the distance between the reservoir pressure and saturation pressure is at a minimum in the reservoir column. Another interesting aspect of the phenomenon is that GOC is exactly at the critical point where properties of gas and liquid are the same, and it is apparent that no distinct discontinuity of properties from liquid to gas occurs. This phenomenon has been reported in several fields as pointed out previously (Schulte, 1980; Creek and Schrader, 1985; Huang, 1985; Hoier et al., 2004). For a detailed discussion about undersaturated GOC systems, case studies and production strategies from these systems refer to Hoier et al. (2004).

2.3.2 Capillary Effect

It is assumed that the interfacial curvature has no practical effect on fluid PVT and VLE for typical sand packing used in the laboratory. However, for in-situ reservoir conditions, it is possible to have quite high interfacial curvature with pore radius in the order of about 1 micron (Lee, 1989). Under such a condition, the capillarity effect was found to become appreciable. A lower reservoir temperature can also make the capillarity effect more pronounced. By neglecting the capillary force, the theory would always predict a sharp GOC and complete gravity segregation for the in-situ fluid phases at discovery conditions.

Wheaton in 1991 presented a thermodynamic theory and formulation for compositional variation with depth. The formulation includes the capillary pressure effect for fluids in the transition zone. However, the factor of interfacial curvature, which is solely responsible for the two-phase separation in the transition zone, was not considered in the equation for thermodynamic equilibrium, namely Eq. (31) of the above referred work.

Among the published works that address the effect of capillarity alone, Sigmund et al. (1973) presented experimental data and theoretical calculations for binary gas condensate systems under the influence of capillarity. The effect was examined by fixing a phase composition and comparing the compositions of the other equilibrium phase under different packings of bead sizes. Sigmund et al.'s results indicate that the effect of interfacial curvature on fluid VLE was insignificant for practical packings of porous media. On the other hand, Trebin and Zadora (1968) reported that experimental dew point pressures of gas condensate mixtures in porous media were 10 to 15 % higher than those observed in conventional PVT cells.

Lee (1989) developed a calculation model to include the capillary pressure in the CG calculations and to do so he has assumed:

1. The system is isothermal and at thermodynamic and mechanical equilibrium.
2. Leverett's J function (1940) is used for representing the curvature function of a reservoir fluid-rock system.

Based on this model, Nikpoor and Chen (2013) developed a mathematical algorithm needed to use Lee's model, they showed how the capillary pressure is introduced into phase behavior calculations.

Chapter Three: **Net Heat of Transport**

3.1 Introduction

In this chapter we elaborate on the nonisothermal CG model, Eq. (2.4). We show where the equation has come from which is important to understand every term in this equation. We introduce the concept of net heat of transport (NHT) and show the models proposed in the literature to calculate this term; and finally choose one model to be used in this study.

3.2 Derivation of the nonisothermal CG model

In a nonisothermal reservoir there always is a heat diffusion from warmer to colder regions, this irreversible phenomenon induces a molecular diffusion in the reservoir (Soret effect) as Onsager's theory states (Onsager, 1931a, b; Kempers, 1989). In a petroleum reservoir with no horizontal temperature gradients (the concept can be applied for the case when there is a horizontal temperature gradients as Faissat et al. showed in 1994) the entropy generation per unit time ad volume can be written as (De Groot, 1951):

$$\sigma = -\frac{1}{T^2}\vec{J}_q \frac{dT}{dh} - \frac{1}{T}\sum_{i=1}^{n_c} \vec{J}_i \left[\frac{T}{M_i} \frac{d\left(\mu_i/T\right)}{dh} - \vec{g} \right] \tag{3.1}$$

where $\vec{J}_q$ is heat flux, $\vec{J}_i$ molar diffusion of component *i* relative to the center of mass velocity. The chemical potential term in Eq. (3.1) can be differentiated to:

$$T\frac{d\left(\mu_i/T\right)}{dh} = \frac{d\mu_i}{dh} - \frac{\mu_i}{T}\frac{dT}{dh} \tag{3.2}$$

From the relationships is the classic thermodynamics:

$$d\mu_i = -\bar{S}_i dT + \bar{v}_i dP + \sum_{j=1}^{n_c} \left(\frac{d\mu_i}{dz_j} \right) dz_j \tag{3.3}$$

where $\bar{S}_i$ is the partial molar entropy of component *i*, $\bar{v}_i$ the partial molar volume of component *I* and z_j the mole fraction of component *j*.

The change in the chemical potential may be devided into a term $((d\mu_i)_T)$ evaluated at constant *T* and a term expressing the contribution to $d\mu_i$ from the variation in *T*:

$$\left(d\mu_i\right)_T = \bar{v}_i dP + \sum_{j=1}^{n_c}\left(\frac{d\mu_i}{dz_j}\right)dz_j \Rightarrow d\mu_i = \left(d\mu_i\right)_T - \bar{S}_i dT \tag{3.4}$$

Insertion of this expression for $d\mu_i$ inro Eq. (3.2) gives:

$$T\frac{d\left(\mu_i/T\right)}{dh} = \left(\frac{d\mu_i}{dh}\right)_T - \left(\frac{\mu_i}{T} + \bar{S}_i\right)\frac{dT}{dh} \tag{3.5}$$

By the use of the general classic thermodynamic relation

$$\bar{H}_i = \mu_i + T\bar{S}_i \tag{3.6}$$

where $\bar{H}_i$ is the partial molar enthalpy of component *i*, Eq. (3.5) can be simplified to:

$$T\frac{d\left(\mu_i/T\right)}{dh} = \left(\frac{d\mu_i}{dh}\right)_T - \frac{\bar{H}_i}{T}\frac{dT}{dh} \tag{3.7}$$

This expression can be insterted into E. (3.1) to give:

$$\sigma = -\frac{1}{T^2}\left(\vec{J}_q - \sum_{i=1}^{n_c}\frac{\bar{H}_i}{M_i}\vec{J}_i\right)\frac{dT}{dh} - \frac{1}{T}\sum_{i=1}^{n_c}\vec{J}_i\left[\frac{1}{M_i}\left(\frac{d\mu_i}{dh}\right)_T - \vec{g}\right] \tag{3.8}$$

Introducing the heat transferred by heat conduction (total heat transfer minus heat transfer from component flow):

$$\vec{J}'_q = \vec{J}_q - \sum_{i=1}^{n_c}\frac{\bar{H}_i}{M_i}\vec{J}_i \tag{3.9}$$

gives the following simplified expression for the entropy production:

$$\sigma = -\frac{1}{T^2}\vec{J}'_q\frac{dT}{dh} - \frac{1}{T}\sum_{i=1}^{n_c}\vec{J}_i\left[\frac{1}{M_i}\left(\frac{d\mu_i}{dh}\right)_T - \vec{g}\right] \tag{3.10}$$

Since the molar diffusion flux $\vec{J}_i$ is relative to center of mass velocity

$$\sum_{i=1}^{n_c}\vec{J}_i = 0 \Rightarrow \vec{J}_{n_c} = -\sum_{i=1}^{n_c-1}\vec{J}_i \tag{3.11}$$

and the last summation in Eq. (3.10) may be rewritten as:

$$\begin{aligned}
&\sum_{i=1}^{n_c-1}\vec{J}_i\left[\frac{1}{M_i}\left(\frac{d\mu_i}{dh}\right)_T - \vec{g}\right] + \vec{J}_{n_c}\left[\frac{1}{M_{n_c}}\left(\frac{d\mu_{n_c}}{dh}\right)_T - \vec{g}\right] \\
&= \sum_{i=1}^{n_c-1}\vec{J}_i\left[\frac{1}{M_i}\left(\frac{d\mu_i}{dh}\right)_T - \vec{g}\right] - \sum_{i=1}^{n_c-1}\vec{J}_i\left[\frac{1}{M_{n_c}}\left(\frac{d\mu_{n_c}}{dh}\right)_T - \vec{g}\right] \\
&= \sum_{i=1}^{n_c-1}\vec{J}_i\left[\frac{1}{M_i}\left(\frac{d\mu_i}{dh}\right) - \frac{1}{M_{n_c}}\left(\frac{d\mu_{n_c}}{dh}\right)\right]_T
\end{aligned} \tag{3.12}$$

This enables the gravitation term $\vec{g}$ to be eliminated from Eq. (3.10) and as a result:

$$\sigma = -\frac{1}{T^2}\vec{J}'_q\frac{dT}{dh} - \frac{1}{T}\sum_{i=1}^{n_c-1}\vec{J}_i\left[\frac{1}{M_i}\left(\frac{d\mu_i}{dh}\right) - \frac{1}{M_{n_c}}\left(\frac{d\mu_{n_c}}{dh}\right)\right]_T \tag{3.13}$$

The following phenomenological relations exist for heat and component fluxes (De Groot, 1951):

$$\vec{J}'_q = -L'_{qq}\frac{\frac{dT}{dh}}{T^2} - \frac{1}{T}\sum_{i=1}^{n_c-1}L'_{qi}\left[\frac{1}{M_i}\left(\frac{d\mu_i}{dh}\right) - \frac{1}{M_{n_c}}\left(\frac{d\mu_{n_c}}{dh}\right)\right]_T \tag{3.14}$$

$$\vec{J}_j = -L'_{jq}\frac{\frac{dT}{dh}}{T^2} - \frac{1}{T}\sum_{i=1}^{n_c-1}L_{ji}\left[\frac{1}{M_i}\left(\frac{d\mu_i}{dh}\right) - \frac{1}{M_{n_c}}\left(\frac{d\mu_{n_c}}{dh}\right)\right]_T \tag{3.15}$$

where L'_{qq}, L'_{qi}, L'_{jq} and L_{ji} are the phenomenological or Onsager coefficients (Onsager, 1931a, b). In the actual context the Onsager coefficients are unpractical to work with since only limited experimental data exist enabling these coefficients to be quantified (Ghorayeb and Firoozabadi,

2000c). For this reason it is desiarable to have Eqs. (3.14) and (3.15) rewritten in terms of other quantities. Shifting to matrix notation, these two equations can be written as:

$$\vec{J}'_q = -L'_{qq}\frac{\frac{dT}{dh}}{T^2} - \frac{1}{T}\left[L'\right]^T\left[\nabla_T\right] \tag{3.16}$$

$$\left[J\right] = -\left[L'\right]\frac{\frac{dT}{dh}}{T^2} - \frac{1}{T}\left[L\right]\left[\nabla_T\right] \tag{3.17}$$

where the superscript *T* shows the transpose operation and:

$$\left[J\right] = \begin{bmatrix} \vec{J}_1 \\ \vec{J}_2 \\ \dots \\ \vec{J}_{n_c-1} \end{bmatrix} \tag{3.18}$$

$$\left[\nabla_T\right] = \begin{bmatrix} \left[\frac{1}{M_1}\left(\frac{d\mu_1}{dh}\right) - \frac{1}{M_{n_c}}\left(\frac{d\mu_{n_c}}{dh}\right)\right]_T \\ \left[\frac{1}{M_2}\left(\frac{d\mu_2}{dh}\right) - \frac{1}{M_{n_c}}\left(\frac{d\mu_{n_c}}{dh}\right)\right]_T \\ \dots \\ \left[\frac{1}{M_{n_c-1}}\left(\frac{d\mu_{n_c-1}}{dh}\right) - \frac{1}{M_{n_c}}\left(\frac{d\mu_{n_c}}{dh}\right)\right]_T \end{bmatrix} \tag{3.19}$$

$$\left[L'\right] = \begin{bmatrix} L'_{q1} \\ L'_{q2} \\ \dots \\ L'_{q,n_c-1} \end{bmatrix} \tag{3.20}$$

$$[L]=\begin{bmatrix} L_{11} & L_{12} & \dots & L_{1,n_c-1} \\ L_{21} & L_{22} & \dots & L_{2,n_c-1} \\ \dots & \dots & \dots & \dots \\ L_{n_c-1,1} & L_{n_c-1,2} & \dots & L_{n_c-1,n_c-1} \end{bmatrix} \tag{3.21}$$

Multiplying Eq. (3.17) by $[L]^{-1}$ gives:

$$[L]^{-1}[J]=-[L]^{-1}[L']\frac{\frac{dT}{dh}}{T^2}-\frac{1}{T}[\nabla_T] \tag{3.22}$$

Now, defining matrix *Q* as:

$$[Q]=[L]^{-1}[L'] \Rightarrow [L']=[L][Q] \tag{3.23}$$

enables us to re-write Eq. (3.22) as:

$$[L]^{-1}[J]=-[Q]\frac{\frac{dT}{dh}}{T^2}-\frac{1}{T}[\nabla_T] \tag{3.24}$$

In a stationary reservoir all component fluxes are zero

$$[J]=0 \Rightarrow -[Q]\frac{\frac{dT}{dh}}{T^2}-\frac{1}{T}[\nabla_T]=0 \tag{3.25}$$

This relation between $[Q]$ and the derivatives of chemical potential with respect to depth is valid for a reservoir with a thermal gradient but at stationary conditions.

$[L][Q]$ from Eq. (3.23) may be inserted for $[L']$ in Eq. (3.16) to give:

$$\vec{J}'_q=-L'_{qq}\frac{\frac{dT}{dh}}{T^2}-\frac{1}{T}[Q]^T[L][\nabla_T] \tag{3.26}$$

Note that $[L]^T = [L]$ based on Onsager's reciprocal relationship theory (Onsager, 1931a, b). Multiplying Eq. (3.17) by $[Q]^T$ gives:

$$[Q]^T [J] = -[Q]^T [L'] \frac{\frac{dT}{dh}}{T^2} - \frac{1}{T}[Q]^T [L][\nabla_T] \tag{3.27}$$

Now, if we combine Eq. (3.26) and (3.27), we will have:

$$\vec{J}'_q - [Q]^T [J] = -L'_{qq} \frac{\frac{dT}{dh}}{T^2} + [Q]^T [L'] \frac{\frac{dT}{dh}}{T^2} \tag{3.28}$$

To evaluate the physical significance of $[Q]$, the limiting case with a temperature gradient of zero may be considered:

$$\frac{dT}{dh} = 0 \Rightarrow \vec{J}'_q = [Q]^T [J] = \sum_{i=1}^{n_c - 1} Q_i \vec{J}_i \tag{3.29}$$

If we combine this equation with Eq. (3.9), it is possible to derive the following expression for $\vec{J}_q$ in a field with zero temperature gradient

$$\frac{dT}{dh} = 0 \Rightarrow \vec{J}_q = \sum_{i=1}^{n_c - 1} Q_i \vec{J}_i + \sum_{i=1}^{n_c} \frac{\bar{H}_i}{M_i} \vec{J}_i = \sum_{i=1}^{n_c - 1} Q_i \vec{J}_i + \sum_{i=1}^{n_c - 1} \frac{\bar{H}_i}{M_i} \vec{J}_i + \frac{\bar{H}_{n_c}}{M_{n_c}} \vec{J}_{n_c} \tag{3.30}$$

In a stationary reservoir Eq. (3.11) applies and if we substitute the last term in Eq. (3.30) from Eq. (3.11) we will have:

$$\frac{dT}{dh} = 0 \Rightarrow \vec{J}_q = \sum_{i=1}^{n_c - 1} \left[\frac{\bar{H}_i}{M_i} - \frac{\bar{H}_{n_c}}{M_{n_c}} + Q_i \right] \vec{J}_i \tag{3.31}$$

It is further assumed that there is no heat flux in an isothermal reservoir, i.e. that:

$$\frac{dT}{dh} = 0 \Rightarrow \vec{J}_q = 0 \tag{3.32}$$

then

$$Q_i = \frac{\bar{H}_{n_c}}{M_{n_c}} - \frac{\bar{H}_i}{M_i} \tag{3.33}$$

Let's now show how introduction of the hydrostatic condition into Eq. (3.25) may be used to derive the temperature dependent tem first proposed by Haase (1990). Eq. (3.33) inserted into Eq. (3.25) to give:

$$-\left[\frac{1}{M_i}\left(\frac{d\mu_i}{dh}\right) - \frac{1}{M_{n_c}}\left(\frac{d\mu_{n_c}}{dh}\right)\right] = \left[\frac{\bar{H}_{n_c}}{M_{n_c}} - \frac{\bar{H}_i}{M_i}\right]\frac{\frac{dT}{dh}}{T};\ i = 1,....,n_c \tag{3.34}$$

The Gibbs-Duhem equation may be written as:

$$-S\frac{dT}{dh} + V\frac{dP}{dh} - \sum_{j=1}^{n_c} z_i \frac{d\mu_i}{dh} = 0 \tag{3.35}$$

At isothermal conditions this equation will give:

$$V\frac{dP}{dh} = \sum_{j=1}^{n_c} z_i \left(\frac{d\mu_i}{dh}\right)_T \tag{3.36}$$

In a petroleum reservoir the pressure gradient will be determined by (hydrostatic condition):

$$\frac{dP}{dh} = \rho g \tag{3.37}$$

Let the thermodynamic diffusion force to be defined as:

$$F_i = g - \frac{1}{M_i}\left(\frac{d\mu_i}{dh}\right) \tag{3.38}$$

Introducing Eqs. (3.37) and (3.38) into Eq. (3.36) gives:

$$V\rho g = \sum_{i=1}^{n_n} z_i \left(M_i g - M_i F_i\right) \tag{3.39}$$

Since

$$V\rho g = g\sum_{i=1}^{n_n} z_i M_i \tag{3.40}$$

the following must apply for the hydrostatic condition in Eq. (3.37) to be fulfilled:

$$\sum_{i=1}^{n_n} z_i M_i F_i = 0 \tag{3.41}$$

Combining Eq. (3.38) and (3.34) gives:

$$F_i - F_{n_c} = \left[\frac{\bar{H}_{n_c}}{M_{n_c}} - \frac{\bar{H}_i}{M_i}\right]\frac{dT}{dh}\frac{}{T} \tag{3.42}$$

Multiplying this equation by $z_i M_i$ and summing over all *i*:

$$\sum_{i=1}^{n_n} z_i M_i F_i - F_{n_c}\sum_{i=1}^{n_n} z_i M_i = \frac{dT}{dh}\frac{}{T}\sum_{i=1}^{n_n} z_i M_i \left[\frac{\bar{H}_{n_c}}{M_{n_c}} - \frac{\bar{H}_i}{M_i}\right] \tag{3.43}$$

As may be seen from Eq. (3.41), the first term in Eq. (3.43) equals zero, giving:

$$F_{n_c} = \frac{\sum_{i=1}^{n_n} z_i M_i \left[\frac{\bar{H}_{n_c}}{M_{n_c}} - \frac{\bar{H}_i}{M_i}\right]}{\sum_{i=1}^{n_n} z_i M_i}\frac{dT}{dh}\frac{}{T} = \left[\frac{H}{M} - \frac{\bar{H}_{n_c}}{M_{n_c}}\right]\frac{dT}{dh}\frac{}{T} \tag{3.44}$$

where *H* is the molar enthalpy of the mixture and *M* is the average MW. Inserting this equation into Eq. (3.42) gives:

$$F_i = \left[\frac{H}{M} - \frac{\bar{H}_i}{M_i}\right]\frac{dT}{dh}\frac{}{T} \tag{3.45}$$

Recalling the definition of F_i in Eq. (3.38), this equation may be rewritten as:

$$\left(\frac{d\mu_i}{dh}\right)_T = M_i\vec{g} - M_i\left[\frac{H}{M} - \frac{\bar{H}_i}{M_i}\right]\frac{dT}{dh}\frac{}{T} \tag{3.46}$$

This equation was proposed by Haase (1990). We define the NHT as:

$$Q_i^{net} = M_i \left[\frac{H}{M} - \frac{\bar{H}_i}{M_i} \right] \tag{3.47}$$

Obviously we used the isothermal condition to come with Eq. (3.47) and we used it in the nonisothermal model Eq. (3.46) which may not be the best approach. Different authors have come to different models for defining the NHT, we will review some of these models in the following sections.

Using the definition in Eq. (3.47), Eq. (46) the can be rewritten as:

$$\left(d\mu_i\right)_T = M_i \vec{g} dh - Q_i^{net} \frac{\frac{dT}{dh}}{T} \tag{3.48}$$

and from classic thermodynamics:

$$\left(d\mu_i\right)_T = RT\left[d\ln\left(f_i\right)\right]_T \tag{3.49}$$

where f_i denotes the fugacity of component i in the mixture which can be easily calculated from EOS. Combining Eqs. (3.49) and (3.48) will give the final working equation in nonisothermal CG:

$$d_T \ln\left(f_i\right) = \frac{M_i \vec{g}}{RT} - Q_i^{net} \frac{dT}{RT^2} \tag{3.50}$$

NHT is the heat transported by unit mass of a component at constant temperature; calculation of this parameter, in spite of its simple definition, is very hard and most of the relationships have been developed for binary systems, while petroleum is a mixture of many more components than two. A problem in the calculation of NHT is its dependence on chemical composition and a mechanism of fluid molecular transport. Finally, we should note that the net heat of transport is still unclear and its effect is usually in the direction of neutralizing the gravity effect.

3.3 Relationships Proposed for Calculation of NHT

These relations are commonly based on statistical mechanics and properties of transport phenomena. In this section, we review some of them.

3.3.1 Relations Proposed for Binary Mixtures

A relation was published in 1958 based on Brownian molecular movement of Kirkwood for the liquid phase (Bearman et al.). Based on this theory, with no external field, NHT of component 1 (Q_1^{net}) in binary mixtures can be partitioned into two:

$$Q_1^{net} = Q_{11}^{net} + Q_{12}^{net} \tag{3.51}$$

Q_{11}^{net} shows the average behavior of the total system in equilibrium, while Q_{12}^{net} represents the perturbations exerted on the equilibrium by heat flow, mass flow and the temperature gradient. Bearman et al. derived general relations for the two parts, but considering the mixture as a regular one, a relationship will be simpler (Tyrrell, 1961):

$$\frac{Q_{11}^{net}}{x_2} = \frac{\overline{v_1}\,\overline{v_2}}{2v}\left[\frac{\overline{L_2}}{\overline{v_2}} - \frac{\overline{L_1}}{\overline{v_1}}\right] \tag{3.52}$$

in which $\overline{L_1}$ is energy of vaporization for component *i* from the solution into ideal gas times (-1). Clearly we can show $\overline{L_i}$ by:

$$\overline{L_i} = \overline{h_i} - \overline{h_i^0} \tag{3.53}$$

in which $\overline{h_i^0}$ is the partial ideal gas enthalpy of component *i*. Bearman et al. calculated $\overline{L_i}$ by:

$$\overline{L_i} = \overline{h_i} - \frac{5}{2}RT \tag{3.54}$$

Obviously, they have taken C_P for ideal gas being equal to *2.5R*. The relation for Q_{12}^{net} net (assuming a regular mixture) is (Tyrrell, 1961):

$$\frac{Q_{12}^{net}}{x_2}=\frac{D_2^*-D_1^*}{2v\left(D_2^*+D_1^*\right)}\left\{\overline{v}_1\overline{v}_2\left[\frac{\overline{L}_2}{\overline{v}_2}-\frac{\overline{L}_1}{\overline{v}_1}\right]+2x_1\left(\overline{L}_1\overline{v}_1-L_1v_1\right)+2x_2\left(\overline{L}_2\overline{v}_2-L_2v_2\right)-I\right\} \qquad (3.55)$$

where *v* is a molar volume at system conditions, $\bar{v}$ a partial molar volume, and *L* molar latent heat of vaporization of components to ideal gas times (*-1*). In the original paper, *L* is calculated by:

$$L_i=h_i-\frac{5}{2}RT \qquad (3.56)$$

"*I*" is an integral containing radial distribution functions in perturbed and unperturbed states and its calculation for real systems is very difficult or impossible. D_1^* and D_2^* are self-diffusion coefficients.

There are a couple of other discussions for determination of the binary mixture NHT, but as we are dealing with multicomponent mixtures, they are irrelevant and neglected. In the next section we review some of the widely-used model for calculation of multicomponent NHT.

3.3.2 Relations Proposed for Multicomponent Mixtures

In recent years several relations have been proposed for multicomponent mixtures. Most of them are generalizations of binary mixture equations, and the most famous of these models are as follows.

3.3.2.1 Haase Relationship

This relation (Haase et al., 1971; Haase and Haase, 1990) has been found assuming a zero temperature gradient (and as a result, a zero heat flux). Consider Eq. (3.47) chapter and after simple mathematical manipulations:

$$Q_i^{net} = \frac{1}{M_m}\left[M_i H_m - M_m \overline{H}_i \right] \tag{3.57}$$

where $\overline{H}_i$ is the partial molar enthalpy, M is the molecular weight, and m represents mixture molar-averaged properties as below:

$$H_m = \sum_{i=1}^{n} x_i \overline{H}_i \tag{3.58}$$

$$M_m = \sum_{i=1}^{n} x_i M_i \tag{3.59}$$

3.3.2.2 Kempers Relationship

This relationship is stated as (Kempers, 1989):

$$Q_i^{net} = \frac{1}{V_m}\left[\bar{v}_i H_m - v_m \overline{H}_i \right] \tag{3.60}$$

where $\bar{v}_i$ is the partial molar volume, H_m as before and v_m is the mixture molar volume defined as:

$$v_m = \sum_{i=1}^{n} x_i \bar{v}_i \tag{3.61}$$

3.3.2.3 Belery-da Silva Relationship

This equation (Belery and da Silva, 1990) is a generalization of the Dougherty and Drickamer (1955) equation (for binary mixtures) to multicomponent mixtures.

$$Q_i^{net} = -\frac{1}{2\hat{v}}\left[\bar{v}_i \Delta u_m^* - v_m \Delta u_i^* \right] \tag{3.62}$$

where

$$\hat{v} = \frac{M_m}{\sum_{i=1}^{n}\left(M_i / \bar{v}_i \right)} \tag{3.63}$$

and Δu_i^* is the partial activation energy of the component *i* which is calculated as:

$$\Delta u_i^* = \left[\frac{\partial \left(n \Delta U_i^* \right)}{\partial n_i} \right]_{P,T,n_{k \neq i}} \tag{3.64}$$

where *n* is the total mole number, n_i is the mole number of component *i*, and ΔU_i^* is a function of viscosity-density ratio defined by the following equation:

$$\Delta U_i^* = R \left\{ \left[\frac{\partial \ln \left(\mu / \rho \right)}{\partial \left(1/T \right)} \right]_{P,x_i} - PT \left[\frac{\partial \ln \left(\mu / \rho \right)}{\partial \left(1/P \right)} \right]_{T,x_i} \right\} \tag{3.65}$$

All other mixture properties are calculated as before.

3.3.2.4 Shukla-Firoozabadi Relationship

This relation (Firoozabadi et al., 2000) is also a generalized equation in the form of:

$$Q_i^{net} = -\frac{\Delta \overline{U}_i}{\tau_i} + \left[\sum_{j=1}^{n} \frac{x_j \Delta \overline{U} j}{\tau_j} \right] \frac{\bar{v}_i}{\sum_{j=1}^{n} x_j \bar{v}_j} \tag{3.66}$$

In this relationship, $\Delta \overline{U}_i$ is called partial molar internal energy departure which is the difference of partial molar internal energy of component *i* in the mixture from its ideal gas state (Creek and Schrader, 1985); $\tau_i = \frac{\Delta U_i^{vap}}{\Delta U_i^{vis}}$ where ΔU_i^{vap} is latent heat of vaporization, and ΔU_i^{vis} is energy of viscous flow. The authors mentioned that τ for binary mixtures can be assumed to be equal to 4. This is based on this fact that at normal boiling point, $ln(\mu)$ is linear versus $1/T$ in a large temperature interval. Constant 4.0 gives good results for calculation of heat diffusion in binary mixtures. Shukla and Firoozabadi stated that this parameter at low pressures can change between 1.0 and 9.0, and calculation of the exact value needs calculation of pure component viscosities (which are not EOS type parameters) at a range of *P* and *T* encountered in the CG calculations.

We have to estimate it usually with a ±*30%* error, which greatly frustrates any attempt to find exact values of τ. The best decision is to accept 4.0 and this is a source of error in the method. However, they showed that the method is still fine.

3.4 Choosing a Suitable Equation for NHT

Several models have been presented in the previous sections to calculate the NHT of components in a multicomponent mixture. The first two (Haase et al., 1971; Haase and Haase, 1990; Kempers, 1989) need knowledge of absolute enthalpy at a reference state which needs optimization and is time-consuming. The third model (Belery and da Silva, 1990) involves determination of parameters difficult to tackle. In this study, we have used the fourth model (Firoozabadi et al., 2000) which does not have problems of the previous alternatives.

We have used 4.0 for parameter τ as the authors have not suggested anything else for multicomponent mixtures; this assumption highly simplifies the calculations. The chosen equation shows that for binary mixtures, lighter component tends toward a warmer zone neglecting gravity (e.g., in a horizontal system subjected to a temperature gradient). All the parameters in this equation are calculated using the PR EOS.

3.5 Calculation of NHT in the Chosen Model

Partial molar internal energy in Shukla-Firoozabadi's (2000) model is calculated from EOS; it is, in fact, residual internal energy:

$$\Delta\overline{U}_i = \overline{U}_i^{\,R} = \overline{H}_i^{\,R} - P.\overline{v}_i^{\,R} \qquad (3.67)$$

where superscript *R* shows a residual property, and the line accent shows a partial molar property. These can be calculated from:

$$\overline{H}_i^{\,R} = -RT^2 \frac{\partial \ln \varphi_i}{\partial T} \qquad (3.68)$$

$$\bar{v}_i^{\,R} = \bar{v}_i - RT/P \tag{3.69}$$

where φ_i denotes the fugacity coefficient of each component in the mixture.

In this chapter we have given a simple proof for the nonisothermal CG model and reviewed the models for calculation of NHT. We have picked a model for NHT calculation and showed how to calculate the necessary terms in the chosen NHT model.

Chapter Four: **Plus Fraction Properties Changes with Depth**

4.1 Introduction

Petroleum fluids consist of infinitely many components, and the usual practice is to report the mole fractions of several pure (and pseudo-) components, lump the remaining heavier part in one single pseudo-component, and call it as a plus fraction. It is obvious that this plus fraction will be a mixture of infinitely many components. Most of the time one treats the plus fraction as a pseudo-component with fixed physical properties in all the calculations involving an EOS but in reality, the same factors leading to compositional variation in a reservoir can change the relative amounts of components within the plus fraction mixture and, therefore, the plus fraction MW and other properties change with respect to location in the reservoir.

Suppose that the plus fraction is composed of components 1 and 2 with different MW's. The average MW of this plus fraction at two depths h^0 and h can be calculated as follows:

$$M^{h^0} = \frac{x_1^{h^0} M_1^{h^0} + x_2^{h^0} M_2^{h^0}}{x_1^{h^0} + x_2^{h^0}} \tag{4.1}$$

$$M^{h} = \frac{x_1^{h} M_1^{h} + x_2^{h} M_2^{h}}{x_1^{h} + x_2^{h}} \tag{4.2}$$

The CG theory states that the mole fractions (x_1 and x_2) change from depth h^0 to h (i.e., the relative amounts of components 1 and 2 in the lumped mixture changes) which leads to a change in the plus fraction MW (as an average) and the EOS properties of the plus fraction will change with respect to location in the reservoir as well.

There are two works in the literature modeling this change (Lira-Galeana et al., 1994; Nia and Movagharnejad, 2007). The work by Lira-Galeana et al (1994) is developed for isothermal reservoirs and it needs complicated calculations and input data which are very difficult to access

which makes it inapplicable for being used in the petroleum reservoir simulation initialization phase; Nia and Movagharnejad (2007) on the other hand made some simplifying assumptions in their derivations (one is the ideal solution assumption) and derived their model to be used only for the case of C_{7+}, they ddn't handle higher plus fractions (C_{8+}, C_{9+}, …).

We assume the same two factors used in the CG modeling in this work (gravity and thermal diffusion) with the same stationary assumption in developing a new model to predict the plus fraction MW change in the reservoir. We use continuous thermodynamics that treats the plus fraction as a mixture of infinitely many components described by a continuous concentration distribution function (CDF) and the same theory of irreversible processes used in the CG study to develop this model. At the same time, we also design a new strategy to model the sharp change in the plus fraction MW that is usually observed at GOC, this sharp change has not been modeled before to the best of our knowledge.

4.2 Continuous Thermodynamics

Composition of petroleum fluids is usually shown by a few discrete fractions; however, the reality is that petroleum fluids are complex mixtures of pure components of continuous ranges in terms of pure components properties, and this composition can be more precisely shown by a continuous function of independent variables such as boiling point temperature or molecular weight. Such functions are called CDF and can be used instead of discrete components in phase behavior calculations.

In Fig. 4.1 we have drawn concentration distribution of the heavy-end pseudo-components of an oil (Pedersen et al., 1992). It is obvious that a statistical function can define CD of the heavy fractions.

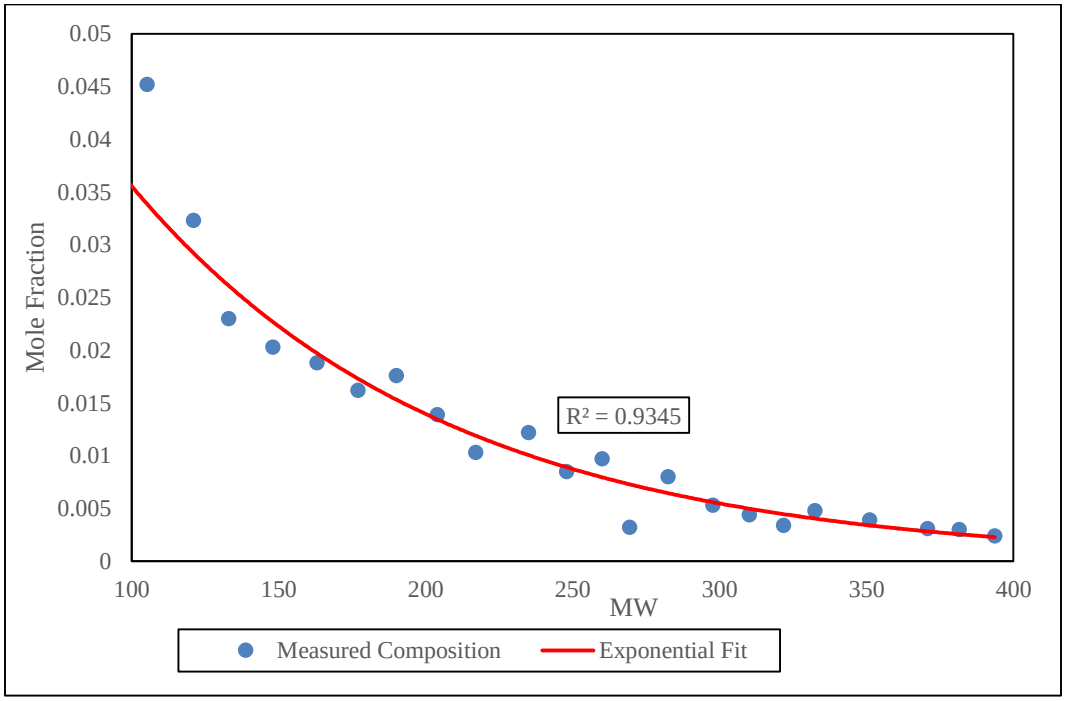

Figure 4.1. CDF of the heavy-end pseudo-components of an oil

The concentration distribution function (CDF) is usually shown by *F(I)* where *I* is the distribution variable (*M*, T_b,…) and satisfies:

$$\int F(I)\,dI = 1, \frac{dx}{dI} = F(I) \tag{4.3}$$

In the integral in Eq. (4.3), the lower and upper bounds for *I* depend on the lower and upper bounds of I within the mixture. The most widely used variables are the MW and carbon number; here we use the MW. It is usually desirable to define the fluid by a semi-continuous scheme where light fractions are shown discretely while heavies are defined by the CDF so that the integral yields the mole fraction of the plus fraction instead of 1.0, i.e.:

$$\int_{\eta}^{\infty} dx = x_{c_+} = \int_{\eta}^{\infty} f(M)\,dM \tag{4.4}$$

where η is the MW of the lightest component within the CDF. Note that f is not equal to F in the sense that F is a normalized f. The average MW of the plus fraction is calculated as follows:

$$\int_{\eta}^{\infty} M dx = x_{c_+} M_{c_+} = \int_{\eta}^{\infty} M f(M) dM \tag{4.5}$$

We need detailed compositional data of heavy fractions to find and match a CDF, and then the CDF can be inserted into EOS calculations. This can greatly reduce the volume of calculations compared with working with a 40 component system which still involves a plus fraction.

The CDF used in this work is the following general gamma function (Manafi et al., 1999):

$$F(M) = \frac{B_{MW}^2}{\eta A_{MW}} \left[\frac{M-\eta}{\eta} \right]^{B_{MW}-1} \exp\left(-\frac{B_{MW}}{A_{MW}} \left[\frac{M-\eta}{\eta} \right]^{B_{MW}} \right) \tag{4.6}$$

where A_{MW} and B_{MW} are the distribution parameters found from matching the function to the detailed compositional data within the plus fraction; as these data are not usually available, we assume B_{MW} as 1.0 and thus the only parameter remaining is A_{MW}. Our distribution function (non-normalized) is of the form:

$$f(M) = \frac{x_{c_+}}{\eta A_{MW}} \exp\left(-\frac{1}{\eta A_{MW}} [M-\eta] \right) \tag{4.7}$$

From Eq. (4.3) we can conclude:

$$dx(M) = f(M) dM \tag{4.8}$$

which shows the mole fraction of a sub-fraction with MW equal to M. On the other hand, from Eq. (3.50) in the previous chapter we can derive the following equation:

$$\left[\frac{\partial \ln(f_k)}{\partial h} \right]_T = \frac{M_k g_h}{RT} - Q_k^{net} \frac{\partial T}{\partial h} \frac{1}{RT^2} \tag{4.9}$$

Consider the definition of a fugacity coefficient:

$$f_i = x_i \varphi_i P \tag{4.10}$$

where φ shows the fugacity coefficient. Now, we substitute this equation for the small sub-fraction as in Eq. (4.8) in Eq. (4.9):

$$\left[dx(M)\varphi(M)P \right]_{T_{avg}}^{h} = \left[dx(M)\varphi(M)P \right]_{T_{avg}}^{h^0} \exp\left(\alpha_G M + \alpha_T\right) \tag{4.11}$$

where

$$\alpha_G = g\left(h - h^0\right) / RT_{avg} \tag{4.12}$$

$$\alpha_T = -Q_M^{net}\left(T - T^0\right) / RT_{avg}^2 \tag{4.13}$$

$$T_{avg} = \left(T + T^0\right) / 2 \tag{4.14}$$

We have introduced the average temperature T_{avg} because the derivative of the fugacity in Eq. (4.9) is at constant temperature and we are using discretization of the reservoir to model the change as the functions cannot be integrated analytically.

From Eq. (4.11) we have:

$$dx(M) = \frac{\left[\varphi(M)P\right]_{T_{avg}}^{h^0}}{\left[\varphi(M)P\right]_{T_{avg}}^{h}} \exp\left(\alpha_G M + \alpha_T\right) dx^{h^0} \tag{4.15}$$

Substituting Eq. (4.8) into this equation yields:

$$dx(M) = \frac{\left[\varphi(M)P\right]_{T_{avg}}^{h^0}}{\left[\varphi(M)P\right]_{T_{avg}}^{h}} \exp\left(\alpha_G M + \alpha_T\right) f^{h^0}(M) dM \tag{4.16}$$

The interesting point about this equation is that integration of both sides, after some mathematical manipulations, will give the same Eq. (4.9) so this formulation is in agreement with the general CG equations.

Considering:

$$x_{c_+}^{h} M_{c_+}^{h} = \int_{\eta}^{\infty} M dx^{h} \tag{4.17}$$

and substitution of Eq. (4.16) into this equation yields:

$$x_{c_+}^{h} M_{c_+}^{h} = \int_{\eta}^{\infty} M \frac{\left[\varphi(M)P\right]_{T_{avg}}^{h^0}}{\left[\varphi(M)P\right]_{T_{avg}}^{h}} f^{h^0}(M) \exp\left(\alpha_G M + \alpha_T\right) dM \tag{4.18}$$

Substituting Eq. (4.7) into Eq. (4.5) yields:

$$M_{c_+}^{h^0} = \eta\left(A_{MW}^{h^0} + 1\right) \tag{4.19}$$

It means that if we have the MW and mole fraction of the plus fraction at depth h^0, we can calculate the distribution parameter A_{MW} at that depth and as a result the CDF by Eq. (4.7) which we insert into Eq. (4.18) to get:

$$M_{c_+}^{h} = \frac{x_{c_+}^{h^0}}{x_{c_+}^{h} \eta A_{MW}^{h^0}} \int_{\eta}^{\infty} M \frac{\left[\varphi(M)P\right]_{T_{avg}}^{h^0}}{\left[\varphi(M)P\right]_{T_{avg}}^{h}} \exp\left(-\frac{1}{\eta A_{MW}^{h^0}}\left[M - \eta\right] + \alpha_G M + \alpha_T\right) dM \tag{4.20}$$

An investigation of the terms in Eq. (4.11) reveals that α_T is much smaller than α_G and because NHT in Eq. (4.13) is very nonlinear with respect to M, we assume α_T to be a constant equal to the plus fraction α_T in Eq. (4.20); furthermore, with good accuracy, we can assume:

$$\frac{\left[\varphi(M)\right]_{T_{avg}}^{h^0}}{\left[\varphi(M)\right]_{T_{avg}}^{h}} = \frac{\varphi_{c_+,T_{avg}}^{h^0}}{\varphi_{c_+,T_{avg}}^{h}} \tag{4.21}$$

to reach the simple integral form:

$$M_{c_+}^{h} = \frac{x_{c_+}^{h^0}\varphi_{c_+,T_{avg}}^{h^0}P^{h^0}}{\eta A_{MW}^{h^0}x_{c_+}^{h}\varphi_{c_+,T_{avg}}^{h}P^{h}}\exp\left(\alpha_T + 1/A_{MW}^{h^0}\right)\int_{\eta}^{\infty} M\exp\left\{\left[\alpha_G - 1/\eta A_{MW}^{h^0}\right]M\right\}dM \qquad (4.22)$$

Integration and simplification give the working equation:

$$M_{c_+}^{h} = \eta\frac{\varphi_{c_+,T_{avg}}^{h^0}}{\varphi_{c_+,T_{avg}}^{h}}\frac{1 + A_{MW}^{h^0} - \alpha_G\eta A_{MW}^{h^0}}{\left(\alpha_G\eta A_{MW}^{h^0} - 1\right)^2}\exp\left(\alpha_G\eta + \alpha_T\right) \qquad (4.23)$$

As a result, we can calculate the variable distribution parameter (A_{MW}) at each depth and can also have changes of the plus fraction molecular weight with depth, whatever the fraction is, but the important point is that η is different for different plus fractions; for C_{7+}, it is the MW of C_6, for C_{8+}, it is the MW of C_7, for C_{9+}, it is the MW of C_8 and so forth. We noticed that Nia and Movagharnejad (2007) had not noticed this important point that taking η always as 84 can severely deteriorate the results and may be interpreted as the weakness of the model, but in general η and A_{MW} are fitting parameters that have to be found from a detailed compositional analysis of the plus fraction.

To involve the plus fraction molecular weight with depth in the CG calculations, we have to have net heat of transport for the plus fraction which itself comes from the general CG calculations; the general CG calculations can be done only when we have MW and other physical properties of the plus fraction so that an iteration is needed with an initial guess to be properties of the plus fraction in the new step equal to those of the previous step. Due to its high nonlinearity, the simultaneous solution of CG and Eq. (4.23) is not recommended.

4.3 Characterization of the Plus Fraction and Important EOS Parameters

We have used the PVTi phase behavior simulation software (Schlumberger, 2005) in order to tune the EOS and obtain all the parameters needed in our subroutines. The other software we used is the Winprop behavior simulation software (Computer Modeling Group Ltd., 2013).

4.4 GOC Detection and Calculation

GOC is the depth at which the fluid mixture changes from a bubble point (P_b) to a dew point (P_d) ($P_{b,Liquid} = P_{d,Vapor}$ at this depth). If the saturation pressure (P_{sat}) at this depth equals the reservoir pressure (instability is detected in CG calculations), then we will observe a conventional saturated GOC where there is a sudden change in density from the gas column to the oil column. Sometimes (especially in near-critical reservoirs) the transition from P_b type to P_d type occurs while the reservoir pressure is higher than the saturation pressure, and hence an undersaturated (stable) GOC occurs; no sharp change is seen and the properties of gas and liquid at this depth are equal, which means the mixture is at its critical temperature (consider the definition of gas and liquid with respect to the critical temperature) at this depth while the saturation pressure matches the critical pressure. It is obvious that a stability analysis can only detect GOCs of the saturated type.

In CG calculation when P_b to P_d transition occurs (between h and h^0), it means that there is a GOC within this depth interval and an interval halving scheme can be used to determine the GOC. If the GOC is saturated (instability is detected at depth h), then a stability analysis can be used to determine the GOC; in the case of an undersaturated GOC,the instability does not occur and a reliable saturation pressure calculation algorithm (as the mixture is near the critical point) is needed.

The method suggested by Hoier and Whitson (2000) seems easy to apply for both types of GOCs. It is described as finding the root of a function D as follows:

$$D\left(h_{GOC}\right) = \Delta_P \times \Delta_K \tag{4.24}$$

where

$$\Delta_P = \left(P - P_{sat}\right) / P \tag{4.25}$$

$$\Delta_K = \sum_{i=1}^{n_c} \left(\ln K_{i,sat}\right)^2 \tag{4.26}$$

and $K_{i,sat}$ are the K-values at the saturation pressure P_{sat}.

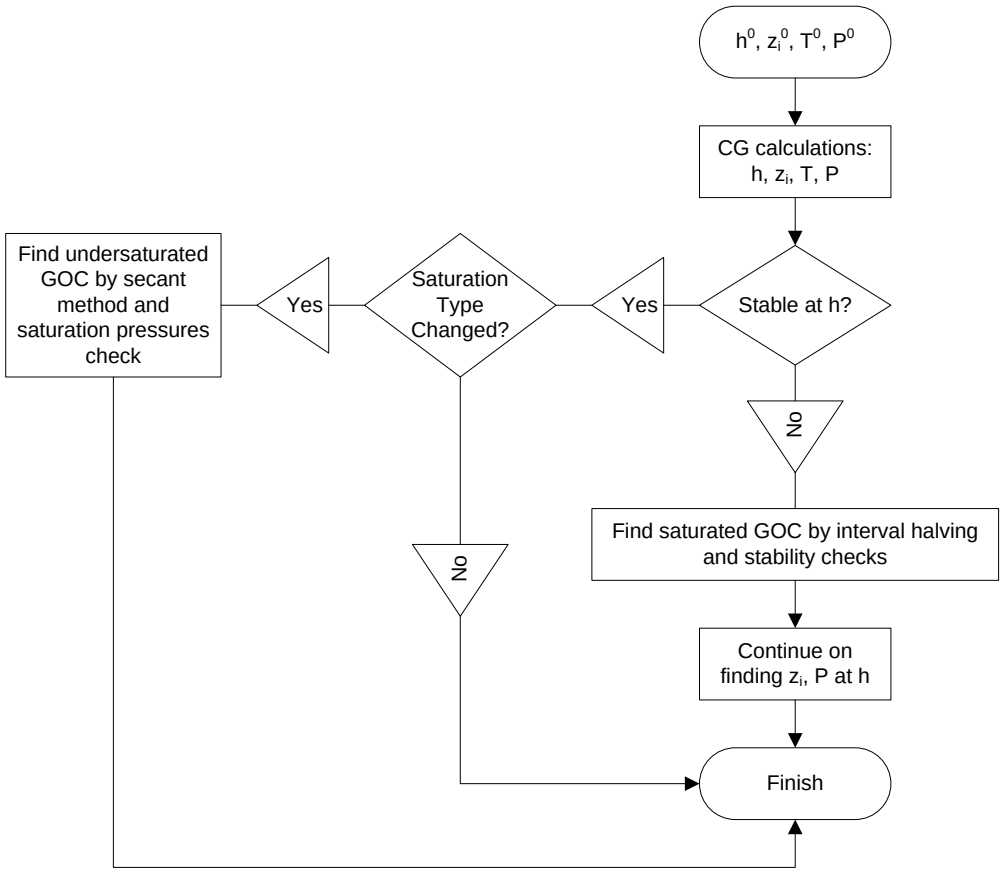

Figure 4.2. The GOC algorithm

A saturated GOC requires the objective function Δ_P to be zero and an undersaturated one requires Δ_K to be zero. The secant method can be used to solve the equations. A simpler algorithm of

detecting and finding the GOC is shown in Fig. 4.2. Note that the MW updating option can be included in the CG-GOC calculations.

4.5 Calculation Scheme

Having the MW of the plus fraction at depth h^0, we first assume that the MW of this fraction for the next step h is the same and do the CG calculations as detailed in the previous sections (knowing T at h and h^0, using the hydraulic equation for P and taking Z^h equal to that at h^0 as the initial guess). We will then have NHT of the plus fraction for the new step which is used to find α_T in Eq. (17) and thus a new estimate of the plus fraction MW for the new step is obtained. Now, we should consider new EOS-related parameters for this fraction at the new step (if required); having the MW and EOS properties of the plus fraction we return to the usual CG calculations again and then update MW and repeat this process until the convergence criteria are met. Note that the gravity term in Eq. (4.12) is calculated using the average plus fraction MW between the two depths:

$$M_{c_+,avg} = \left(M_{c_+}^{h} + M_{c_+}^{h^0} \right) / 2 \qquad (4.27)$$

The flowchart in Fig. 4.3 shows the process.

4.6 Numerical Algorithm

The numerical algorithm used here combines Newton's method for pressure and successive substitution for composition and MW. Note that the volume corrections inside the fugacity equations will not cancel contrary to what we see in case of flash calculations. The reason is the change of pressure from one depth step to the next. This observation should be also included in the fugacity derivatives.

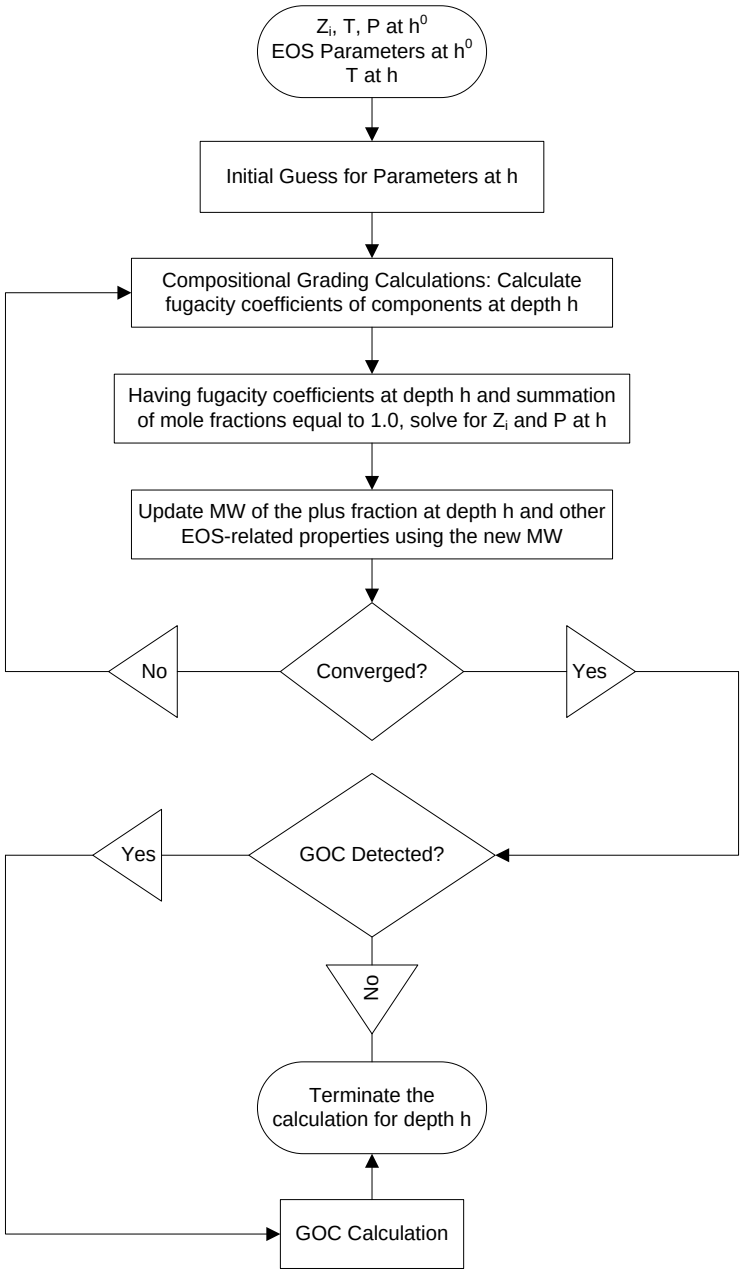

Figure 4.3. CG calculation Algorithm

The algorithm begins with:

$$A_{MW}^{h^0} = \frac{M_{c_+}^{h^0} - \eta}{\eta} \tag{4.28}$$

Then a loop-wise iteration is given as follows (*n* shows the iteration count):

$$\tilde{f}_i^{(n)} = f_{i,T_{avg}}^{h^0} \exp\left[\frac{M_{i,avg}^{(n)} g\left(h-h^0\right)}{RT_{avg}} - \frac{Q_{i,T_{avg}}^{net,(n)}\left(T^h - T^{h^0}\right)}{RT_{avg}^2}\right] \tag{4.29}$$

$$r_i = \frac{\tilde{f}_i^{(n)}}{f_{i,T_{avg}}^{(n)}}\left[\sum_{j=1}^{n_c} Y_j^{(n)}\right]^{-1} \tag{4.30}$$

$$Y_i^{(n+1)} = Y_i^{(n)} r_i \tag{4.31}$$

$$\theta^{(n)}\left(P^{(n)}, Z^{(n)}\right) = \sum_{j=1}^{n_c} Y_j^{(n)} - 1 \tag{4.32}$$

$$P^{(n+1)} = P^{(n)} - \left[\frac{\theta^{(n)}}{\left[\partial\theta / \partial P\right]^{(n)}}\right]_{T_{avg}} \tag{4.33}$$

$$Z_i^{(n+1)} = \frac{Y_i^{(n+1)}}{\sum_{j=1}^{n_c} Y_j^{(n+1)}} \tag{4.34}$$

$$M_{c_+}^h = \eta \frac{\varphi_{c_+,T_{avg}}^{h^0}}{\varphi_{c_+,T_{avg}}^h} \frac{1 + A_{MW}^{h^0} - \alpha_G \eta A_{MW}^{h^0}}{\left(\alpha_G \eta A_{MW}^{h^0} - 1\right)^2} \exp\left(\alpha_G \eta + \alpha_T\right) \tag{4.35}$$

In this equation, the average properties are used as discussed earlier. The derivatives used are obtained as:

$$\frac{\partial\theta}{\partial P} = \sum_{j=1}^{n_c}\left[Y_j r_j \left(\frac{\partial\tilde{f}_j / \partial P}{\tilde{f}_j} - \frac{\partial f_j / \partial P}{f_j}\right)\right] \tag{4.36}$$

$$\frac{\partial\tilde{f}_j}{\partial P} = -\tilde{f}_j \frac{\partial Q_{j,T_{avg}}^{net}}{\partial P} \frac{\left(T^h - T^{h^0}\right)}{RT_{avg}^2} \tag{4.37}$$

Now, a convergence check can be done on any comfortable basis; we recommend the following criteria:

$$|\theta| < 10^{-13} \tag{4.38}$$

$$\left|\underline{r} - 1\right|_{max} < 10^{-13} \tag{4.39}$$

This chapter shows a systematic method to derive a nonisothermal model the plus fraction MW change in the reservoir; we chose the plus fraction CDF to be exponential to derive our model, however, any other model can be equally used while the derivation of the final model will be the same. Furthermore, we have proposed a simple numerical algorithm for the CG modeling to be used in the reservoir simulation initialization, the algorithm involves discretization of the reservoir which is the usual way in the reservoir simulation to build the static model.

Chapter Five: **Model Validation and Case Studies**

5.1 Introduction

In this chapter we validate the model and our computer subroutine (developed via MATLAB) using measured data. We will further run sensitivity analyses to investigate what affects the output of the models and also to study different CG behavior of fluids.

5.2 Case Study 1: Plus Fraction Molecular Weight Change Modeling Validation

Field data used in this work are those used by Schou Pedersen and Hjermstad (2006), and Table 5.1 shows fluid compositions from six different depths in a petroleum reservoir, it also presents some key reservoir data and the sampled compositions including pressure and plus fraction MW variations with depth. The reservoir system consists of an oil column underneath a gas cap. A saturated GOC is located in a depth of 3,647 meter. The two compositions in Table 5.1 from depths above 3,647 m are from the gas zone and the remaining four samples are from the oil zone.

The temperature increases by approximately 0.026 °C per meter vertical depth. With some investigations in the mole fractions of C_1 and C_{10+} we can realize that the amount of difference between the methane (and the plus fraction) concentrations in the liquid and gas columns should be much higher than what Table 5.1 shows; a tuning of EOS and the characterization given in the original paper cannot simulate the liquid-gas equilibrium, and because of experimental measurements, we can clearly see that from the depth of 3,644.3 m to 3,638.2 m the observed C10+ mole fraction increases, and it is against what we should normally see, there are other odd data seen in this table.

Table 5.1. Case study 1, observed Fluid Characteristics with Depth in the Reservoir

Depth (m)	3682.8	3676	3661.6	3651.1	3644.3	3638.2
N2	0.395	0.337	0.331	0.358	0.295	0.431
CO2	2.06	2.363	2.455	2.332	2.834	2.752
C1	53.871	54.253	55.261	56.142	68.546	68.861
C2	7.589	7.961	8.025	8.094	8.341	8.427
C3	5.575	5.494	5.481	5.535	5.212	5.198
iC4	1.009	1	0.995	1.001	0.892	0.847
nC4	2.514	2.454	2.433	2.439	2.1	1.885
iC5	0.9	0.889	0.877	0.879	0.675	0.587
nC5	1.396	1.202	1.182	1.184	0.866	0.752
C6	1.557	1.539	1.504	1.504	0.981	0.921
C7	2.63	2.579	2.52	2.474	1.519	1.482
C8	2.823	2.777	2.667	2.583	1.61	1.595
C9	1.897	1.869	1.779	1.695	1.048	1.031
C10+	15.783	15.282	14.491	13.78	5.08	5.231
P (bar)	380.2	379.6	378.8	378.2	377.9	377.8
C10+ MW	297.2	291.8	284.3	281.6	216.8	211.3

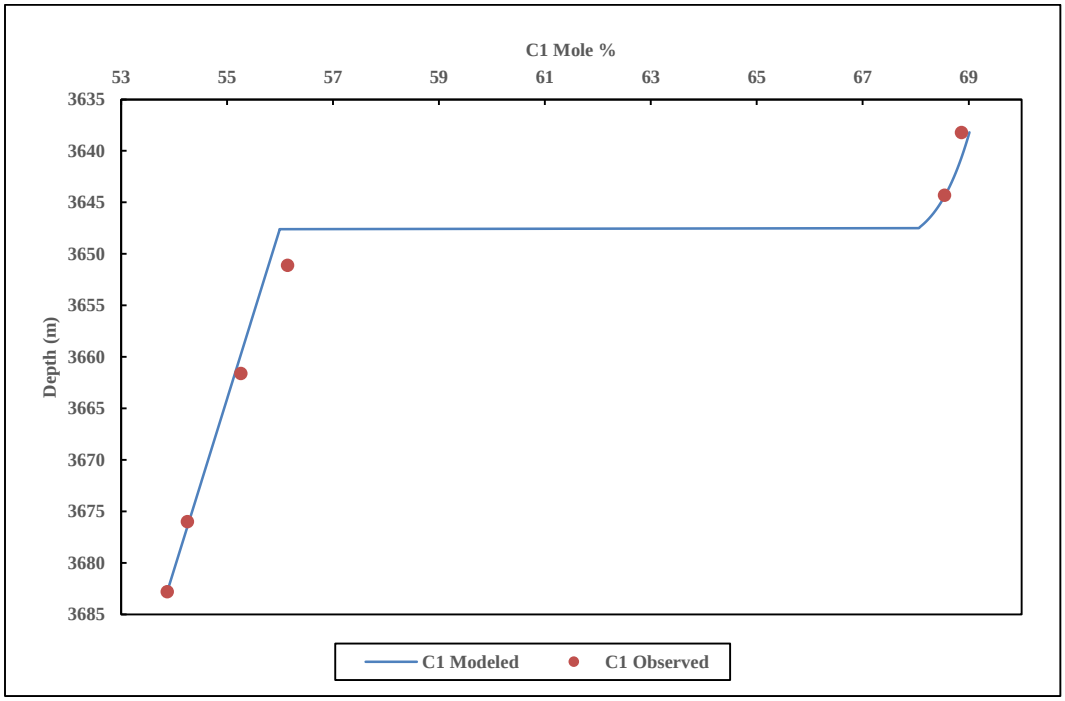

Figure 5.1. Case study 1, C1 mole fraction vs. depth

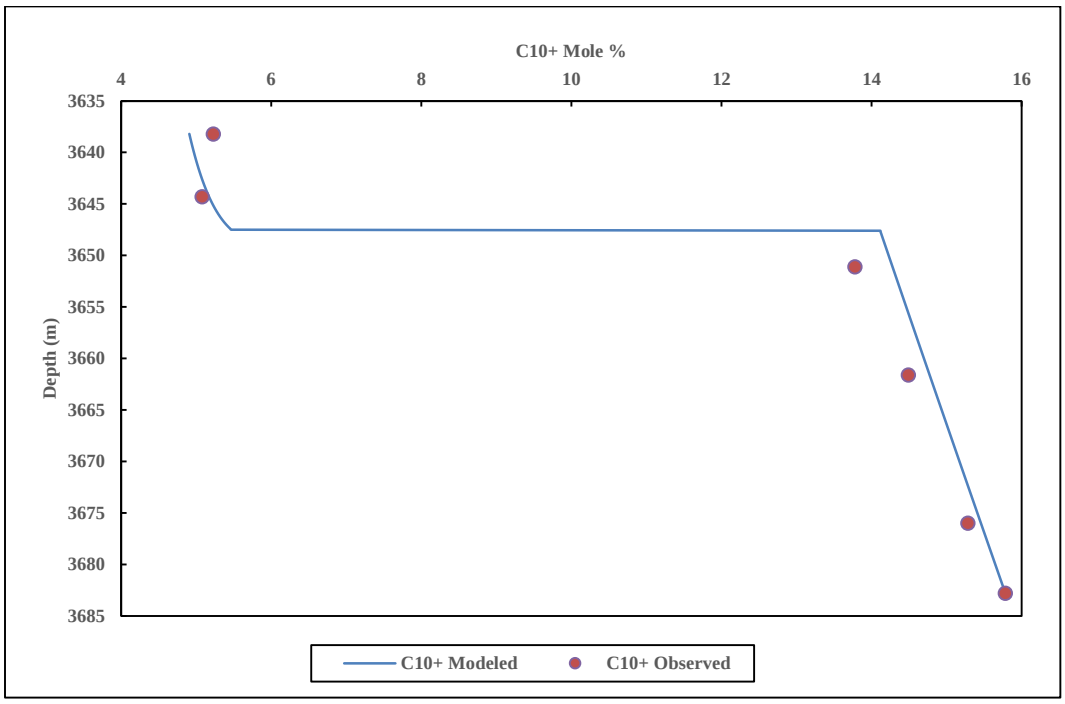

Figure 5.2. Case study 1, C10+ mole fraction vs. depth

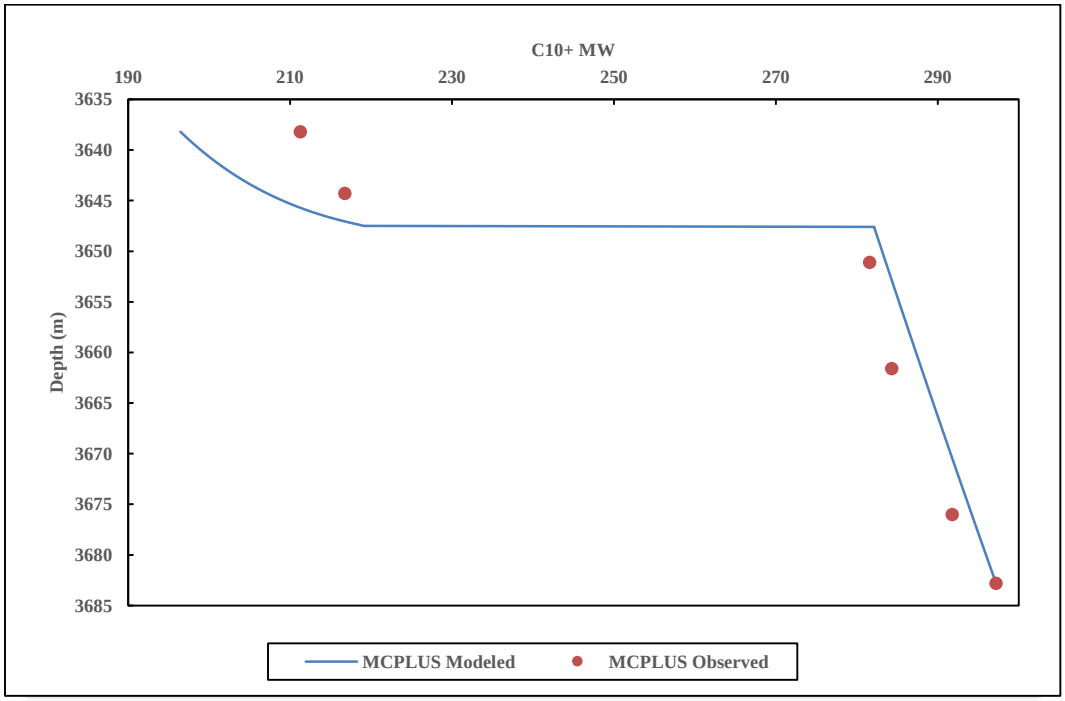

Figure 5.3. Case study 1, C10+ MW vs. depth

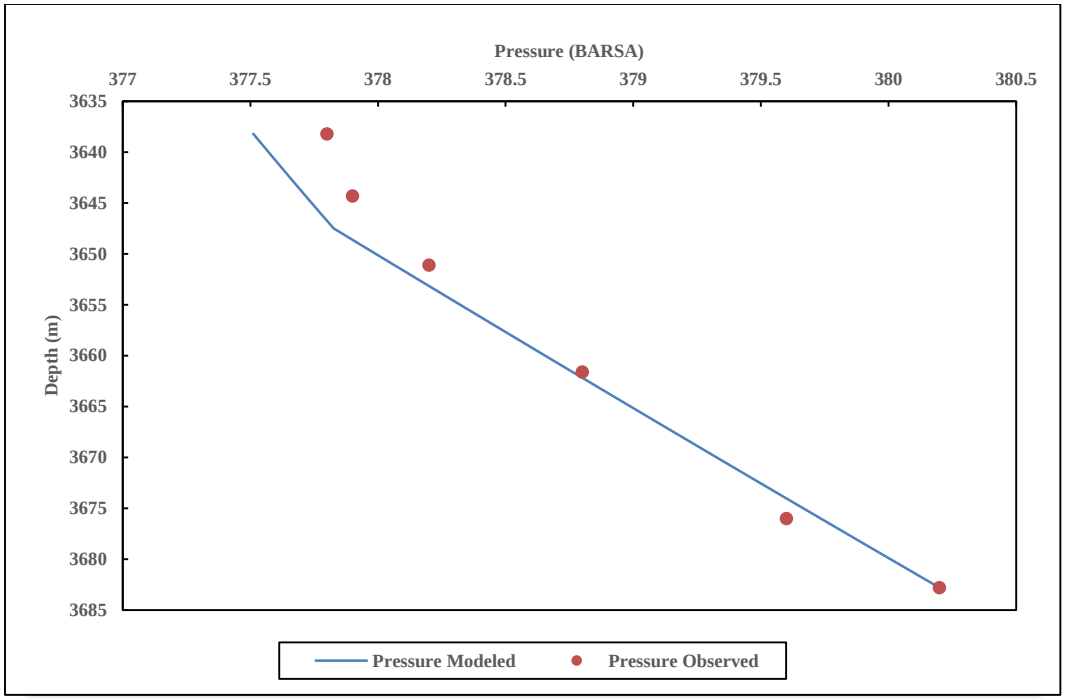

Figure 5.4. Case study 1, pressure vs. depth

The sample at the depth of 3,682.8 m is taken as the reference in this study to calculate properties at the other depths. At the GOC (3,647.5 m depth), the plus fraction is splited into nine subfractions to calculate the incipient phase composition and the sharp change in the plus fraction MW by lumping the subfractions back to a plus fraction, and in each of the two steps the EOS has to be re-tuned. The same CDF is used for splitting as was used for the calculation of changes in the plus fraction MW with depth and the new (split) phase envelope was matched to that of the original lumped one to ensure consistency. Simulation results are summarized in Figs. 5.1-5.4 and Table 5.2; the plus fraction MW change is very well simulated by the model except in the gas column which is due to the unreliable splitting and lumping back.

Figs. 5.3 and 5.4 show that the model under-predicts the compositional gradient in the reservoir under study. The fact that flash calculations cannot simulate the observed vapor-liquid equilibrium

(VLE) under any tuning effort shows that the measured data are under question as Pedersen and Hjermstad mentioned in their work (2006) which means that the EOS is unable to model the fluid behavior and the CG algorithm which has been validated earlier (Nikpoor et al., 2011) cannot match the reported data. Fig. 5.5 shows that the plus fraction MW model works very well in the oil column, and it has not matched the data in the gas column due to the inefficiency of the EOS in modeling VLE at the GOC.

Table 5.2. Case study 1, output of the program

Depth (m)	3682.8	3676	3661.6	3651.1	3644.3	3638.2
N2	0.3950	0.3959	0.3979	0.3993	0.5650	0.5713
CO2	2.0600	2.0610	2.0631	2.0646	2.2835	2.2873
C1	53.8719	53.9746	54.1918	54.3502	68.5565	69.0145
C2	7.5891	7.5971	7.6139	7.6260	7.9566	7.9517
C3	5.5751	5.5786	5.5859	5.5910	5.2923	5.2667
iC4	1.0090	1.0095	1.0104	1.0110	0.8876	0.8804
nC4	2.5140	2.5146	2.5156	2.5162	2.1206	2.1002
iC5	0.9000	0.9000	0.9000	0.8999	0.7120	0.7031
nC5	1.3960	1.3959	1.3956	1.3953	1.0791	1.0647
C6	1.5570	1.5565	1.5555	1.5545	1.0826	1.0634
C7	2.6300	2.6278	2.6229	2.6192	1.6424	1.6065
C8	2.8230	2.8197	2.8123	2.8067	1.6325	1.5919
C9	1.8970	1.8944	1.8887	1.8843	1.0165	0.9879
C10+	15.7830	15.6744	15.4464	15.2817	5.1729	4.9104
P (bar)	380.2000	379.7343	378.7617	378.0639	377.7162	377.5115
C10+ MW	297.2000	294.2014	287.9953	283.5863	207.1992	196.4690

5.3 Case Study 2: Model Validation, a North Sea Reservoir

The reservoir under study is a North Sea Brent reservoir (Montel and Gouel, 1985). We have selected three samples, one for reference state and the other two for validation of the model. Fluid is light oil under a temperature gradient of 0.025 K/m. Measured compositional data are given in Table 5.3 and the other needed data are illustrated in Table 5.3 while results of running the code are shown in Fig. 5.5 and Table 5.4.

Reservoir pressure and temperature at the depth of 3,179.5m are measured to be 397.2 BARSA and 379.8 K, respectively; the fluid density is 458 kg/m^3, and the plus fraction molecular weight is 242.75 g/mol at this depth.

Table 5.3. Case study 2, observed Fluid Characteristics with Depth in the Reservoir

Depth (m)	3162	3179.5	3204.5	3241
N2	0.87	0.64	0.54	0.51
CO2	2.77	2.87	2.75	2.75
C1	68.31	63.14	57.2	53.06
C2	9.52	9.62	9.53	9.84
C3	5.77	5.92	6.33	6.65
C4	2.75	2.86	3.24	3.49
C5	1.45	1.67	2.01	2.25
C6	1.5	2.01	2.51	2.88
C7	1.36	1.99	2.5	2.93
C8	0.94	1.56	1.98	2.31
C9	0.88	0.95	1.61	1.39
C10	0.45	0.64	0.78	0.95
C11+	3.44	6.13	9.02	11

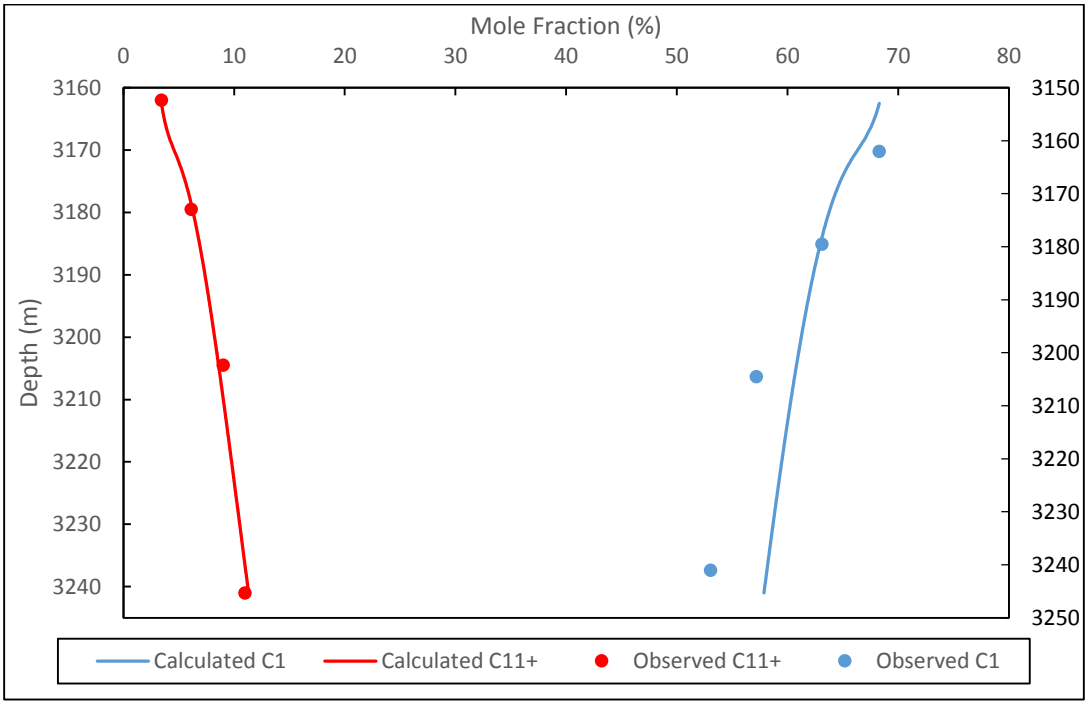

Figure 5.5. Case study 2, composition output of the model compared with observed data

Table 5.4. Case study 2, output of the program

Depth (m)	3162	3179.5	3204.5	3241
N2	0.8699	0.7780	0.7239	0.6766
CO2	2.7697	2.7287	2.6877	2.6383
C1	68.3032	63.8397	60.8136	57.8774
C2	9.5190	9.4703	9.3329	9.1246
C3	5.7694	5.9898	6.0360	6.0017
C4	2.7497	2.9689	3.0540	3.0843
C5	1.4499	1.6305	1.7133	1.7584
C6	1.4999	1.7565	1.8846	1.9643
C7	1.3599	1.6608	1.8242	1.9385
C8	0.9399	1.1849	1.3246	1.4276
C9	0.8799	1.1478	1.3058	1.4260
C10	0.4500	0.6051	0.6992	0.7723
C11+	3.4397	6.2389	8.6002	11.3101

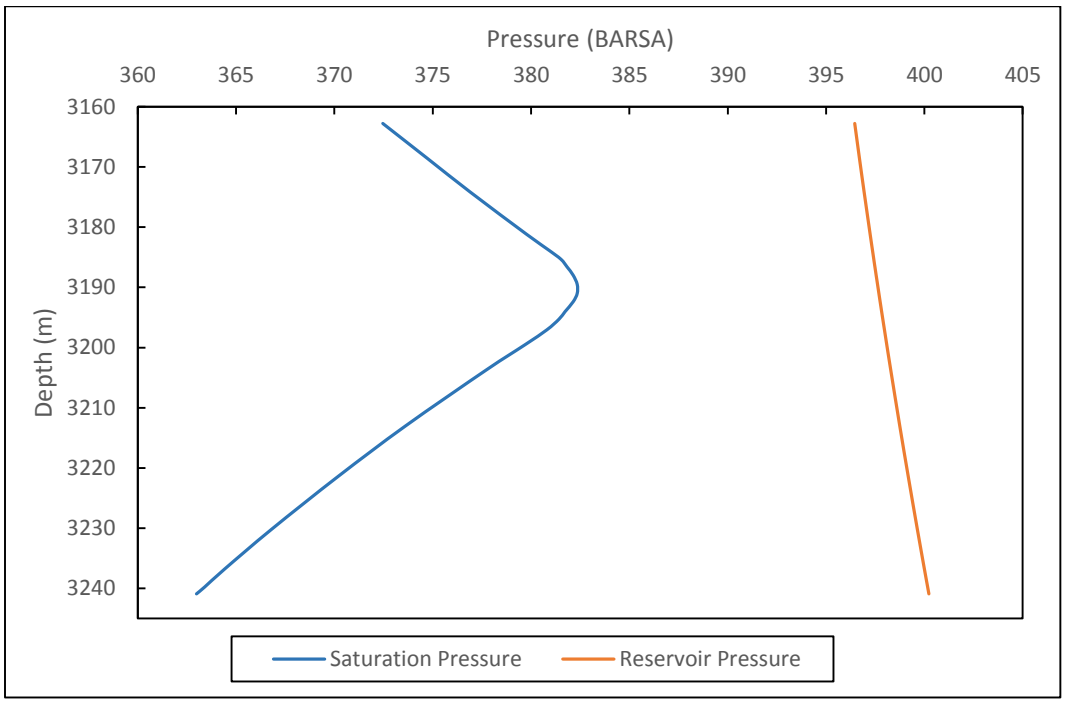

Figure 5.6. Case study 2, reservoir pressure and saturation pressure, showing an undersaturated GOC in the system

As we see, the model can adequately predict the change of fluid composition in the reservoir. This reservoir has an undersaturated GOC and it is detected in this model to be at the depth of 3,194.5 m as shown in Fig. 5.6. This figure shows that the maximum saturation pressure in the reservoir happens at the GOC and it is always below the reservoir pressure.

5.4 Case Study 3: Sensitivity Analysis of CG for a Synthetic Oil

In this section, we have chosen a synthetic oil with the composition and some component properties given in Table 5.5 and the phase envelope in Fig. 5.7. We will assess the effect of different changes on the CG behavior of this oil. The critical pressure and temperature of the fluid are 23.85 MPa and 523.67 K, respectively.

Table 5.5. Case study 3, composition and component properties

Comp.	Mole %	Pc (MPa)	Tc (K)	Acentric Factor	MW	Spgr
CO2	0.90	7.38	304.20	0.23	44.01	0.82
N2	0.30	3.39	126.20	0.04	28.01	0.81
CH4	53.47	4.60	190.60	0.01	16.04	0.30
C2H6	11.46	4.88	305.40	0.10	30.07	0.36
C3H8	8.79	4.25	369.80	0.15	44.10	0.51
IC4	2.13	3.65	408.10	0.18	58.12	0.56
NC4	2.43	3.80	425.20	0.19	58.12	0.58
IC5	1.08	3.38	460.40	0.23	72.15	0.63
NC5	1.01	3.37	469.60	0.25	72.15	0.63
FC6	1.51	3.29	507.50	0.28	86.00	0.69
C7+	16.92	2.17	693.23	0.55	173.00	0.84

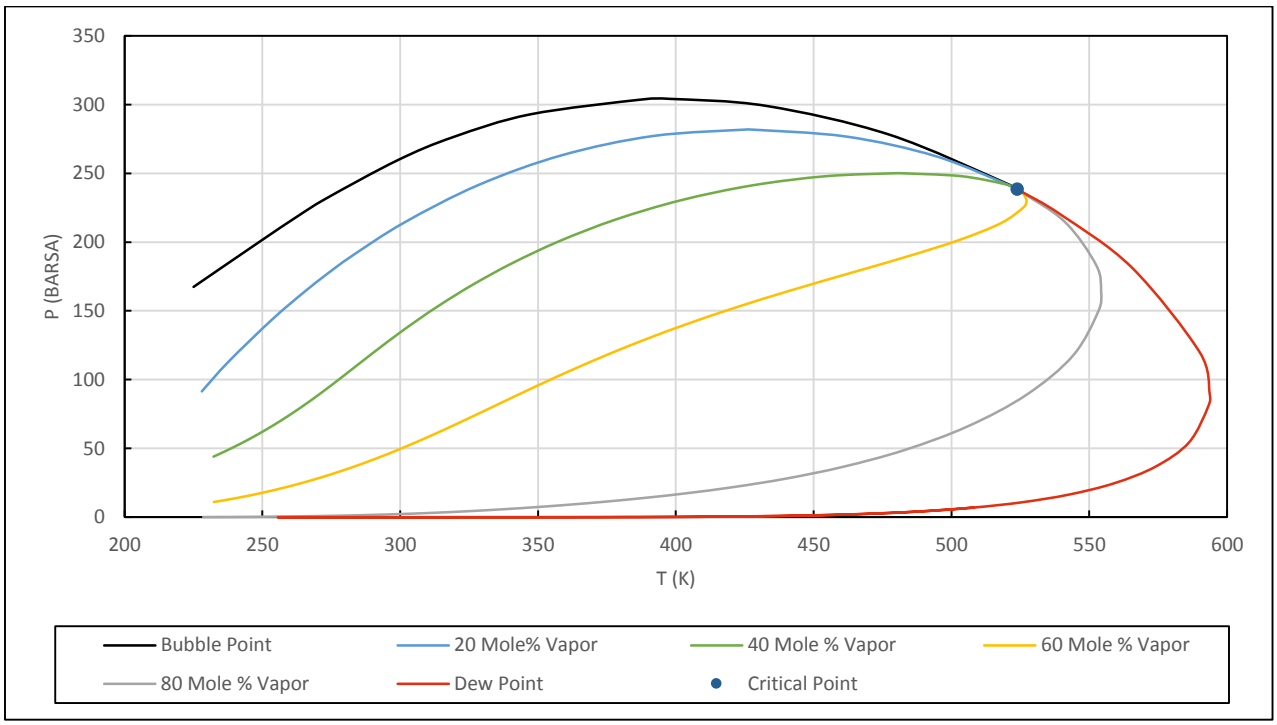

Figure 5.7. Case study 3, phase envelope of the fluid

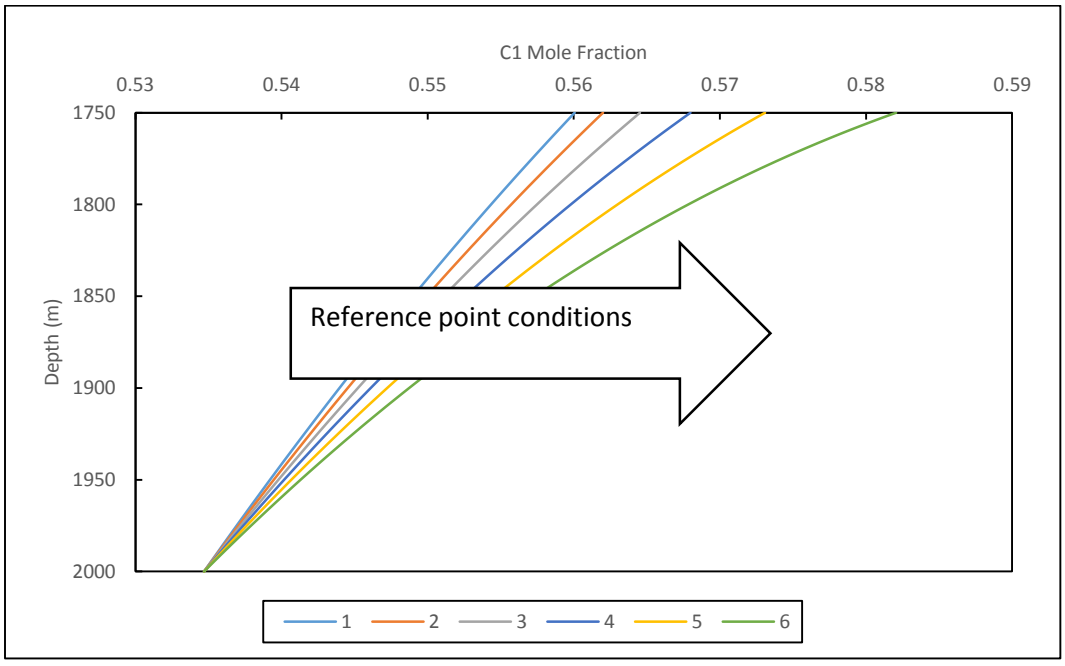

Figure 5.8. Case study 3, methane concentration changes with depth, from 1 to 6, the reference fluid gets closer to the critical point

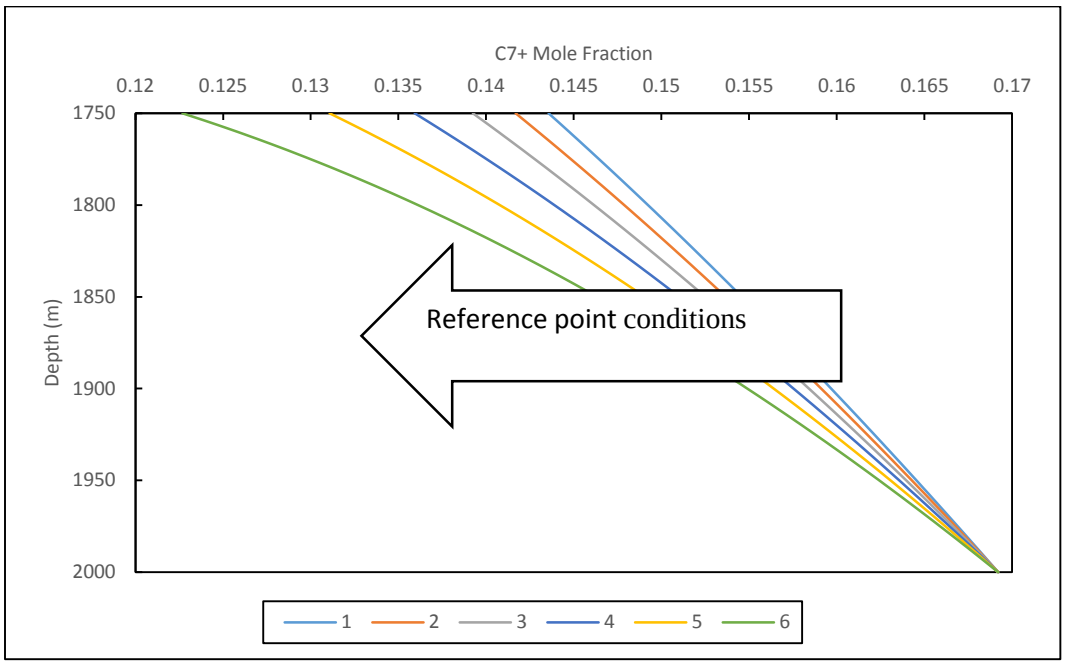

Figure 5.9. Case study 3, heptane plus fraction concentration changes with depth, from 1 to 6, the reference fluid gets closer to the critical point

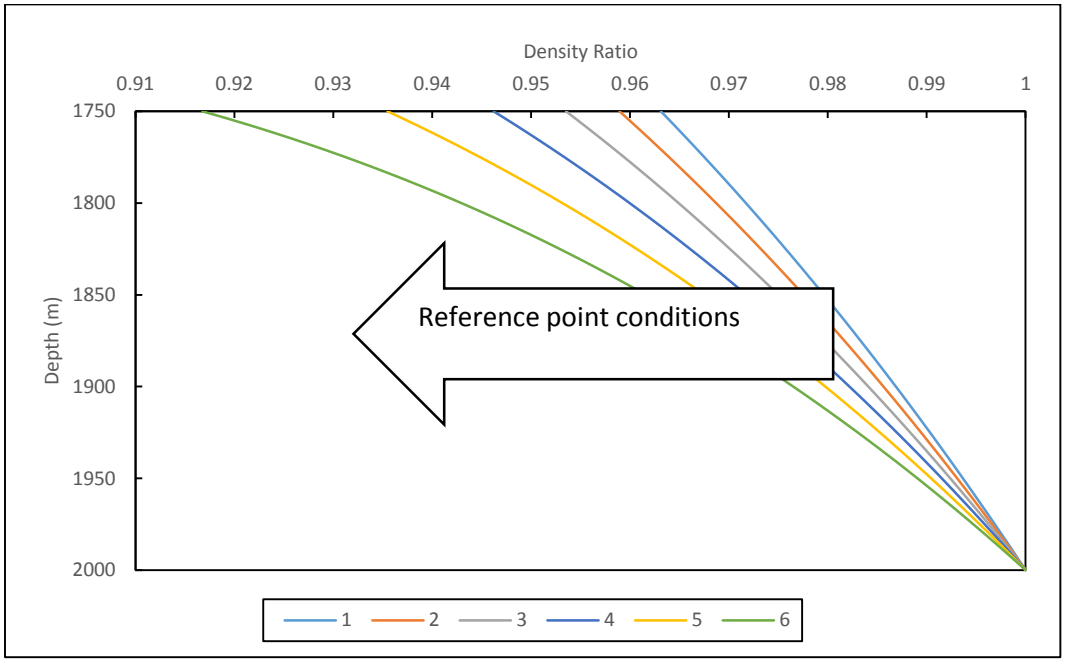

Figure 5.10. Case study 3, density ratio changes with depth, from 1 to 6, the reference fluid gets closer to the critical point

We change the reference conditions and the EOS parameters for the isothermal reservoir case and show the results in Figs. 5.8-5.10. In all of our calculations, we assume the reservoir to be 250 m thick and the reference point at the depth of 2,000 m.

In Figs. 5.8-5.10, from the lines 1 to 6 the reference point gets closer to the critical point and as we see, it results in a more severe and nonlinear gradient in properties. In Fig. 5.10, we have introduced the concept of a dimensionless density ratio which is defined as the density of the fluid divided by that at the reference point, which makes all the lines to start at the same point in the graph.

In Figs. 5.11-5.13, from the lines 1 to 6 we have increased the normal temperature gradient (i.e., temperature increases downwards), and as we can clearly see, the properties gradients decrease, which shows that the thermal diffusion effect is in the direction of cancelling the gravitational effect.

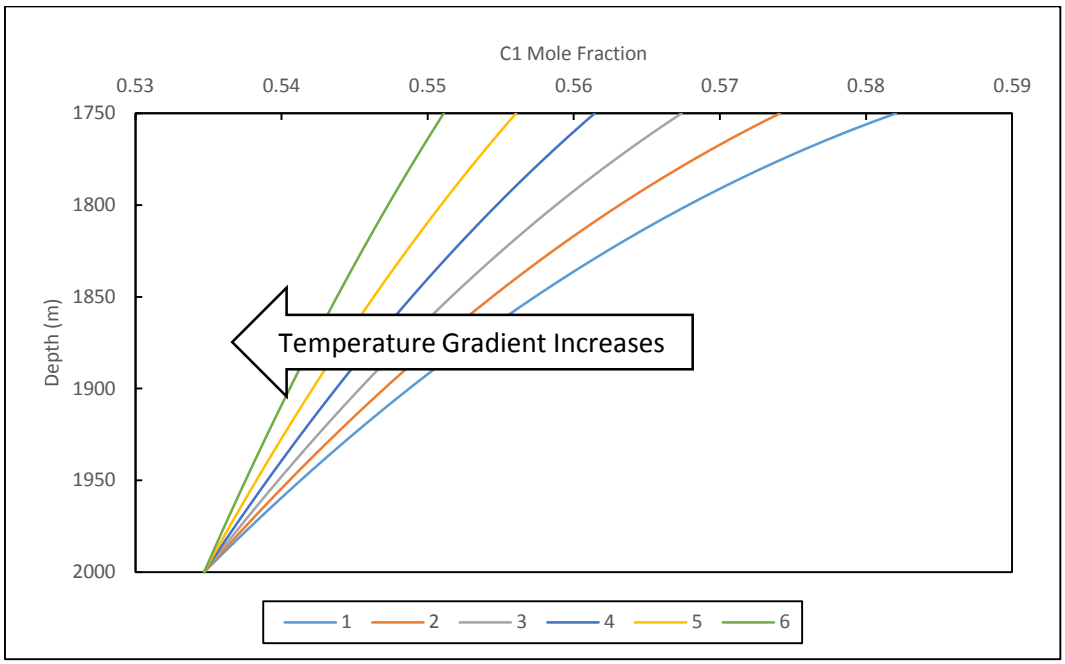

Figure 5.11. Case study 3, methane concentration changes with depth, from 1 to 6 the temperature gradient increases

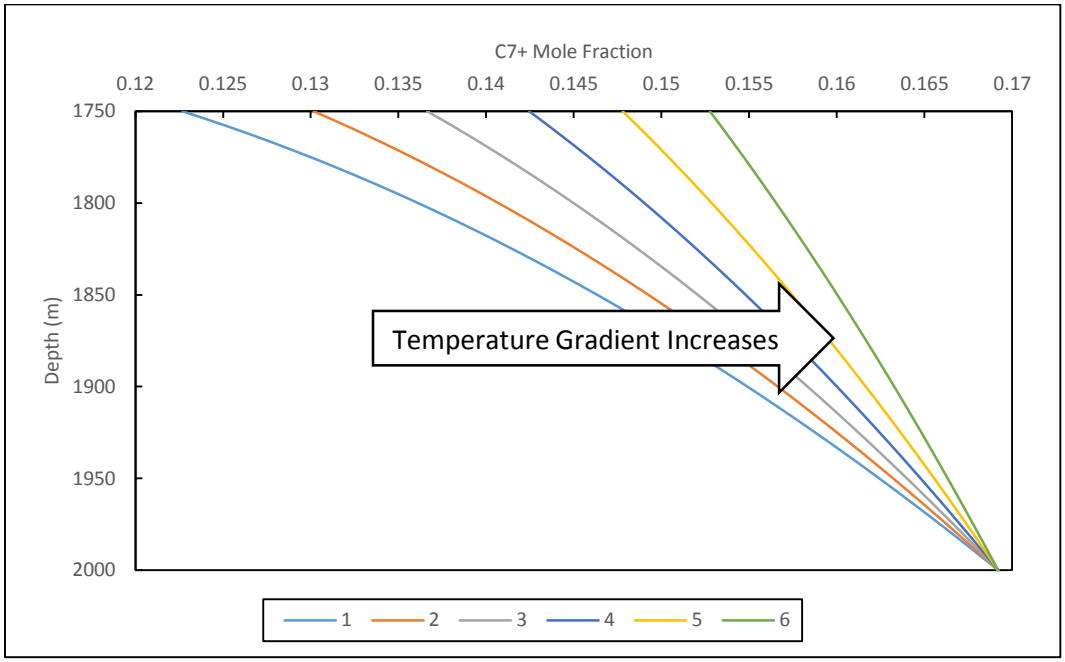

Figure 5.12. Case study 3, heptane plus fraction concentration changes with depth, from 1 to 6 the temperature gradient increases

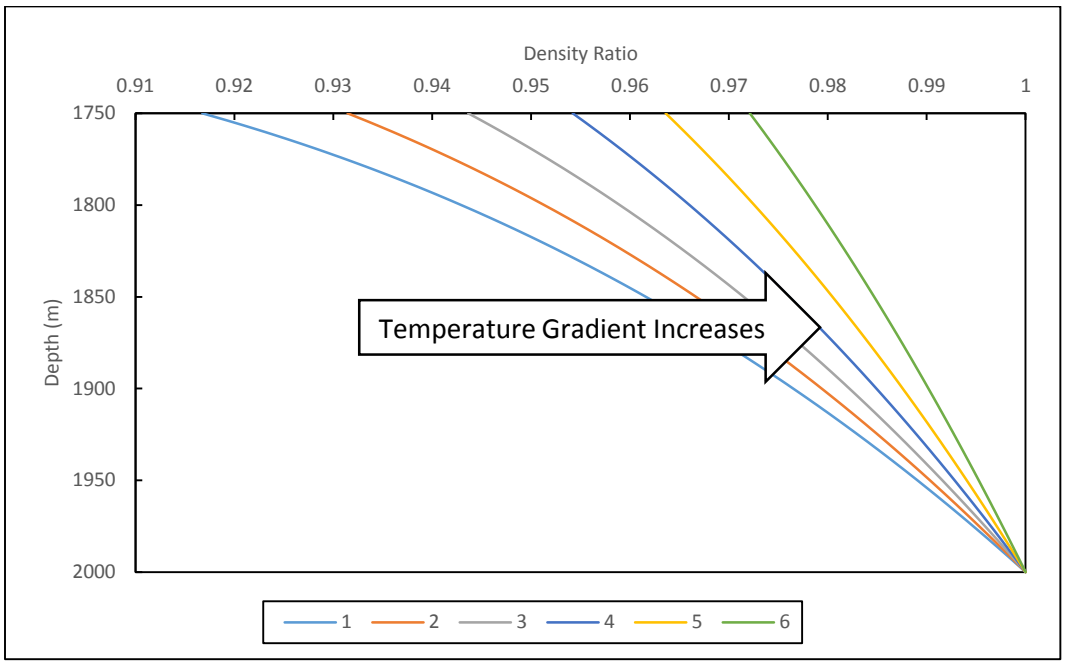

Figure 5.13. Case study 3, density ratio changes with depth, from 1 to 6 the temperature gradient increases

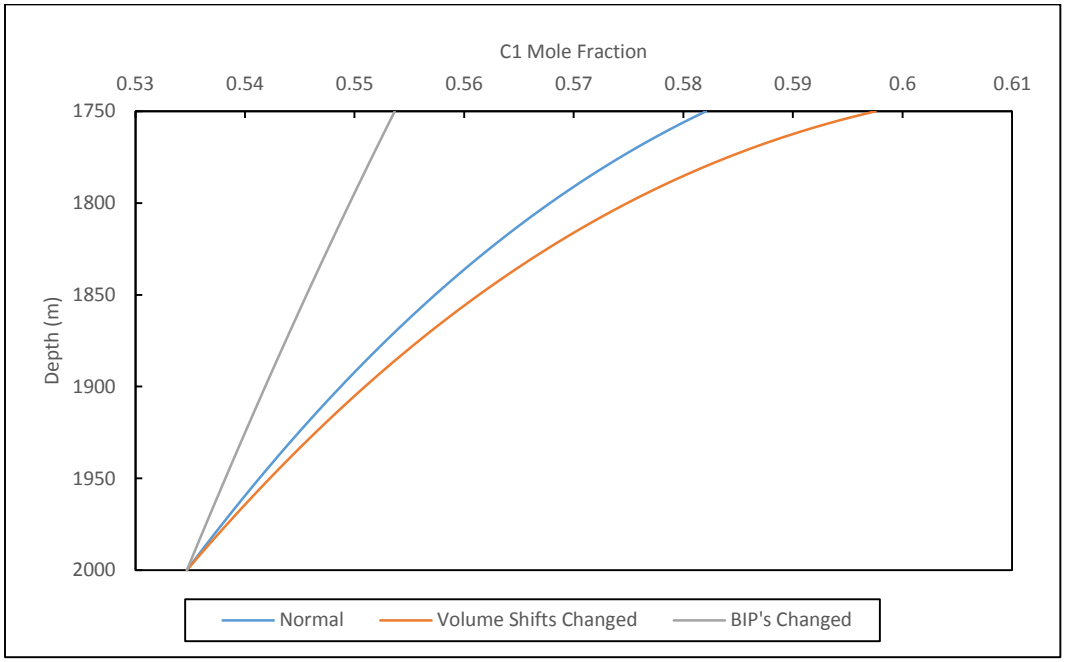

Figure 5.14. Case study 3, methane concentration changes with depth, investigating the effect of volume shifts and BIP's

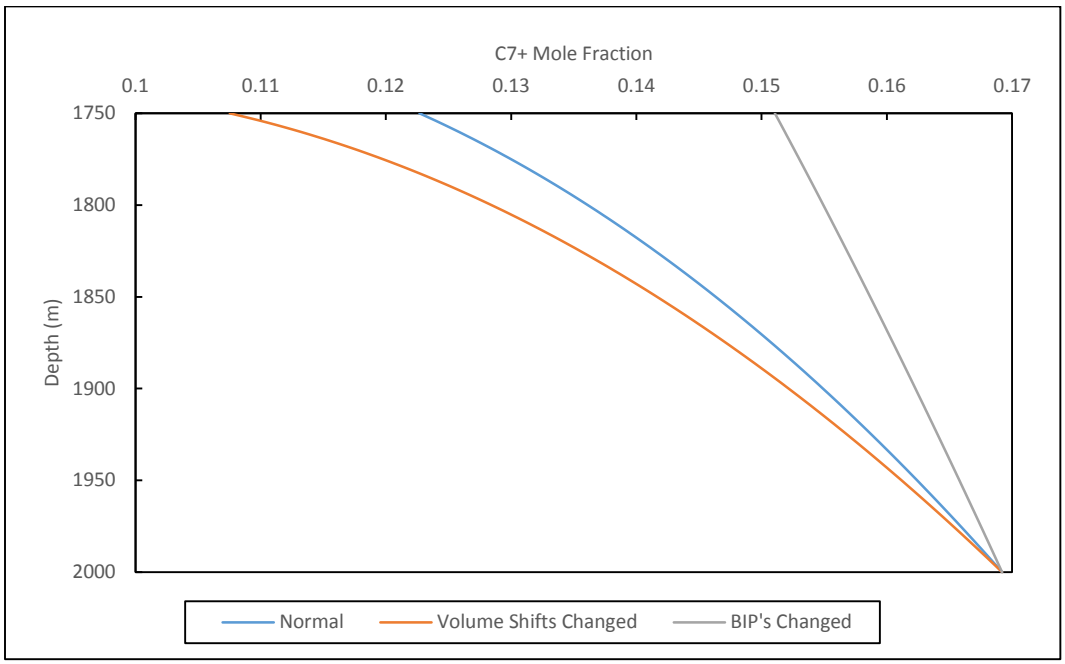

Figure 5.15. Case study 3, heptane plus fraction concentration changes with depth, investigating the effect of volume shifts and BIP's

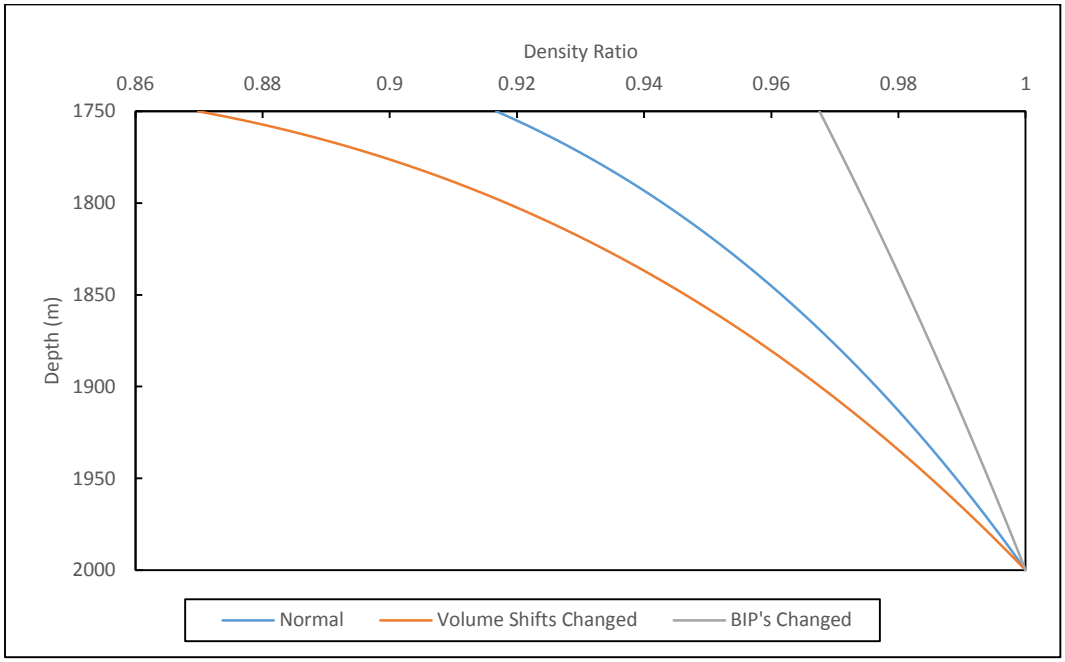

Figure 5.16. Case Study 3, density ratio changes with depth, investigating the effect of volume shifts and BIP's

In Figs. 5.14-5.16, we have changed the volume shifts and binary interaction coefficients separately and independently in the isothermal reservoir, and as we can see, they have a profound effect on the fluid property gradients. Noteworthy is that to change the volume shifts and BIP's we have tuned the EOS to match the same single phase liquid density as we did in case of the volume shifts change but the effects on the CG are totally different. As we can see, the volume shifts affect the CG opposite to what we have seen in case of the flash equilibrium calculations where the volume shifts are canceled out of the calculations.

5.5 Case Study 4: Synthetic Retrograde Gas, Various Fluid Distribution Types

In this section, we have chosen a synthetic retrograde gas reservoir with the fluid composition given in Table 5.6; the reservoir formation continues from 1,750 m to 2,000 m as in the previous section. The sample is chosen to be at the bottom of the reservoir. The phase envelope of the fluid is shown in Fig. 5.17. As shown, the critical temperature and pressure are 296.42 K and 237.99 BARSA, respectively.

Table 5.6. Case study 4, reference fluid composition

Component	Feed MoleFraction	MW	SPgr
CH4	0.73		
C2H6	0.08		
C3H8	0.06		
IC4	0.02		
NC4	0.01		
IC5	0.01		
NC5	0.01		
FC6	0.01		
C7+	0.07	121	0.81

The near-critical condition of retrograde gas reservoirs makes the fluid PVT behavior very sensitive to small changes in *P* and *T* and they show severe CG, which makes the design of production and EOR strategies very difficult. Here, we have chosen the reference *P* and *T* to be

333.15 K and 270 BARSA, respectively, which puts the fluid near the critical region of the fluid as seen in Fig. 5.17.

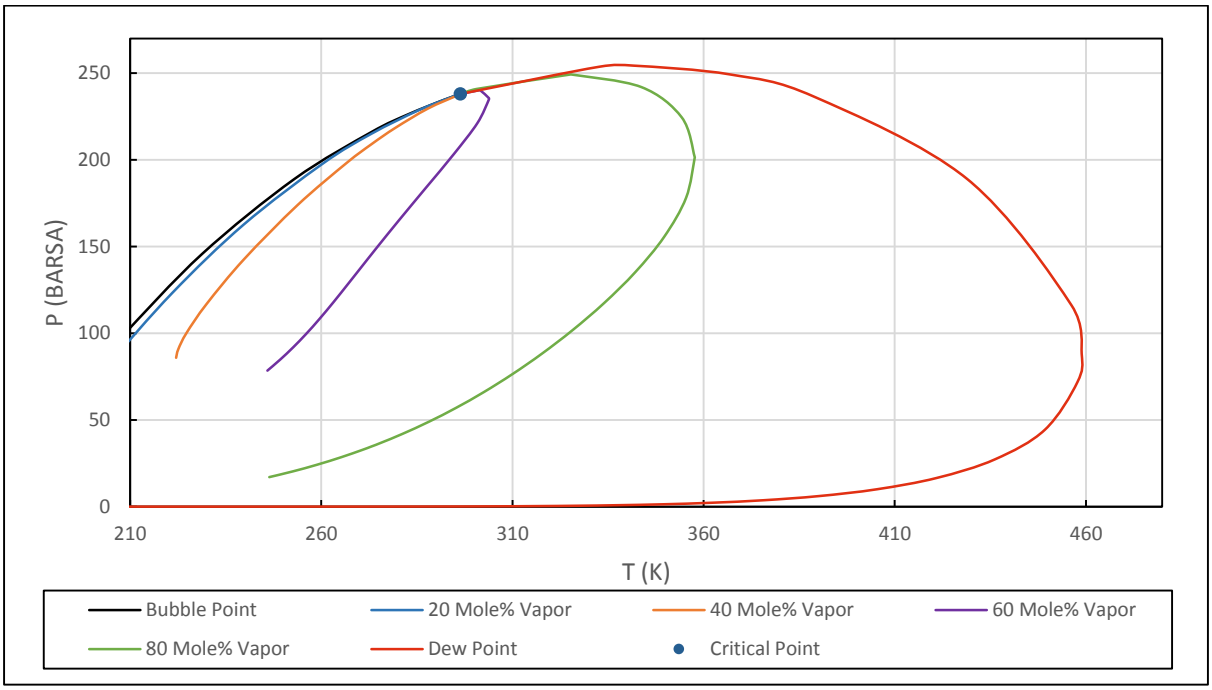

Figure 5.17. Case study 4, phase envelope of the fluid

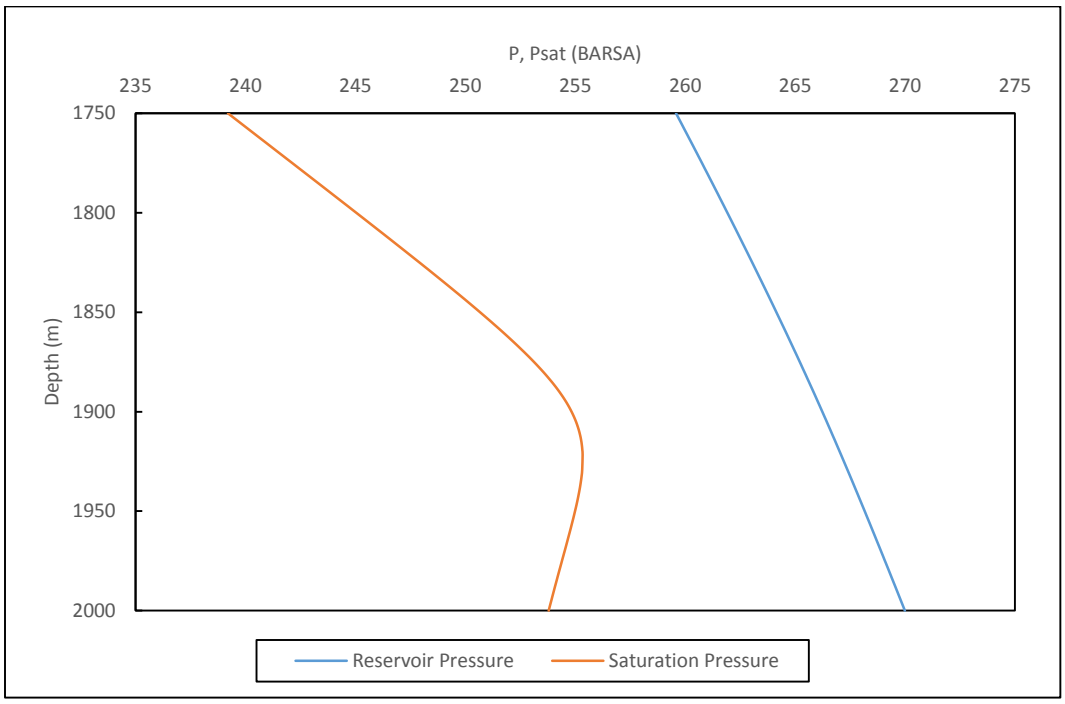

Figure 5.18. Case study 4, undersaturated GOC

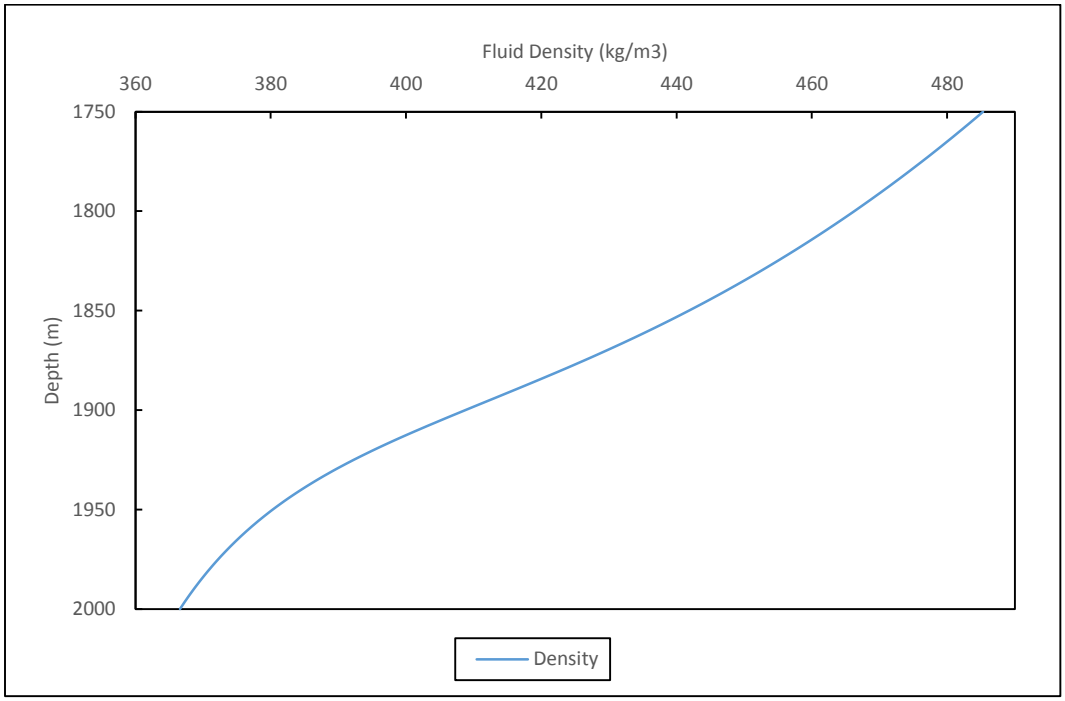

Figure 5.19. Case study 4, unusual fluid density distribution

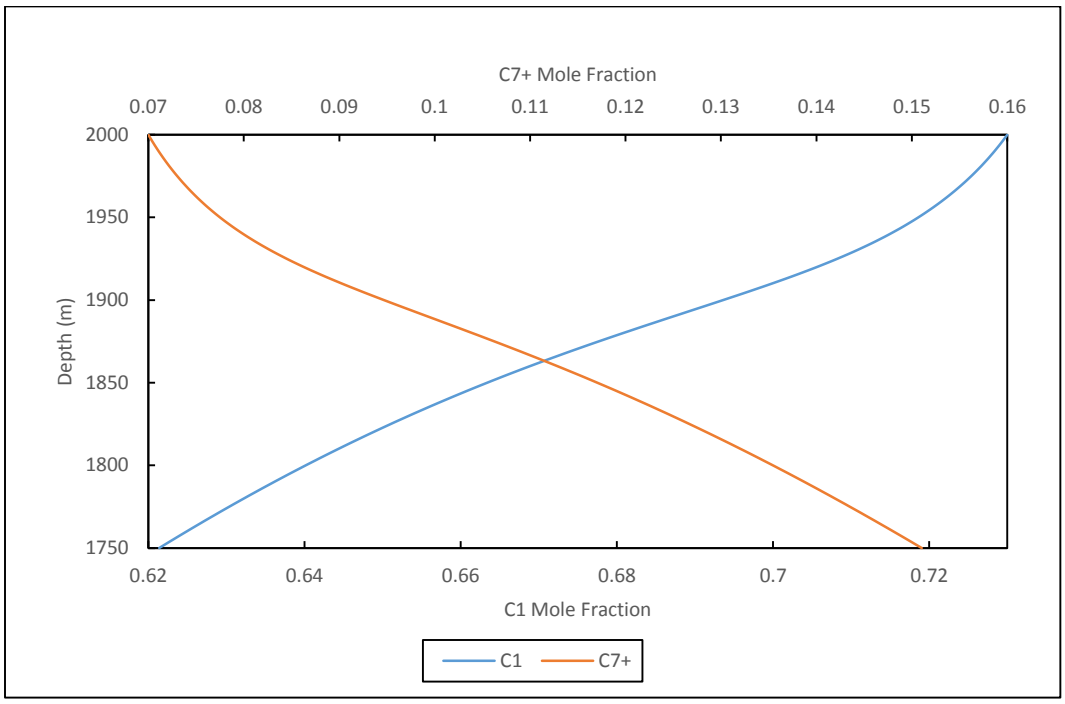

Figure 5.20. Case study 4, unusual component distribution

Now, if we decrease the temperature gradient to 0.001 K/m, we will see the results as in Figs. 5.21-5.23 which is the normal fluid distribution we observe in most of the reservoirs. This discussion clearly shows that the fluid CG becomes more sensitive to the temperature gradient when the fluid conditions approaches to the critical point; under severe conditions, the fluid may show strange distribution patterns in the fluid column.

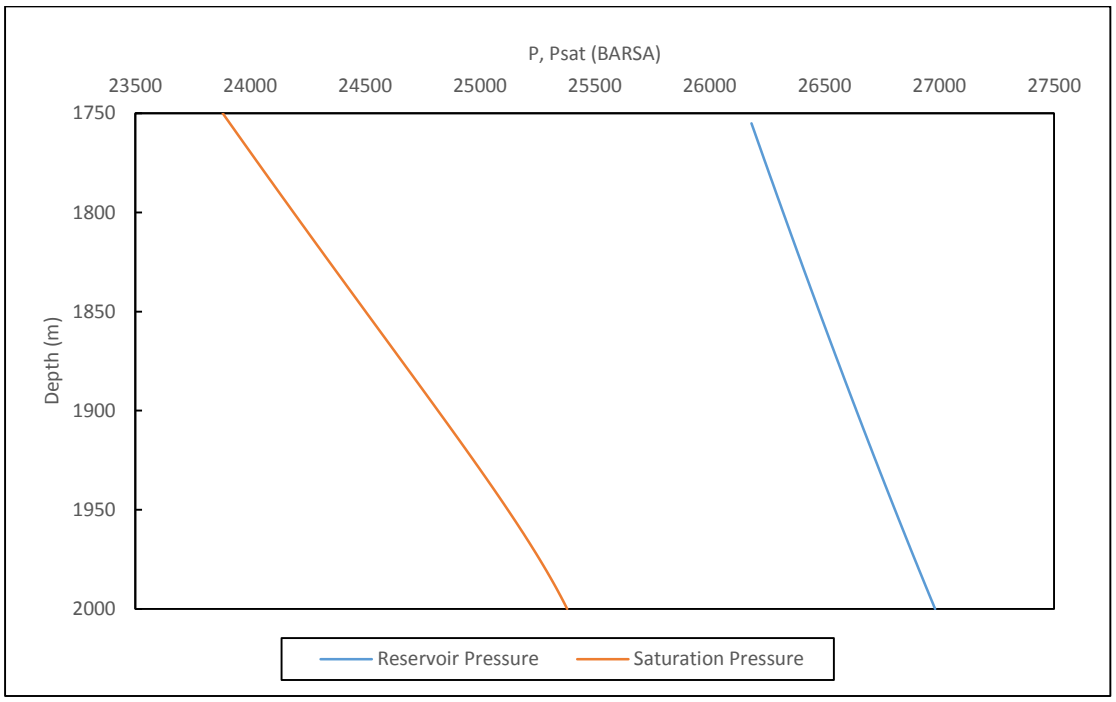

Figure 5.21. Case study 4, undersaturated system with no GOC

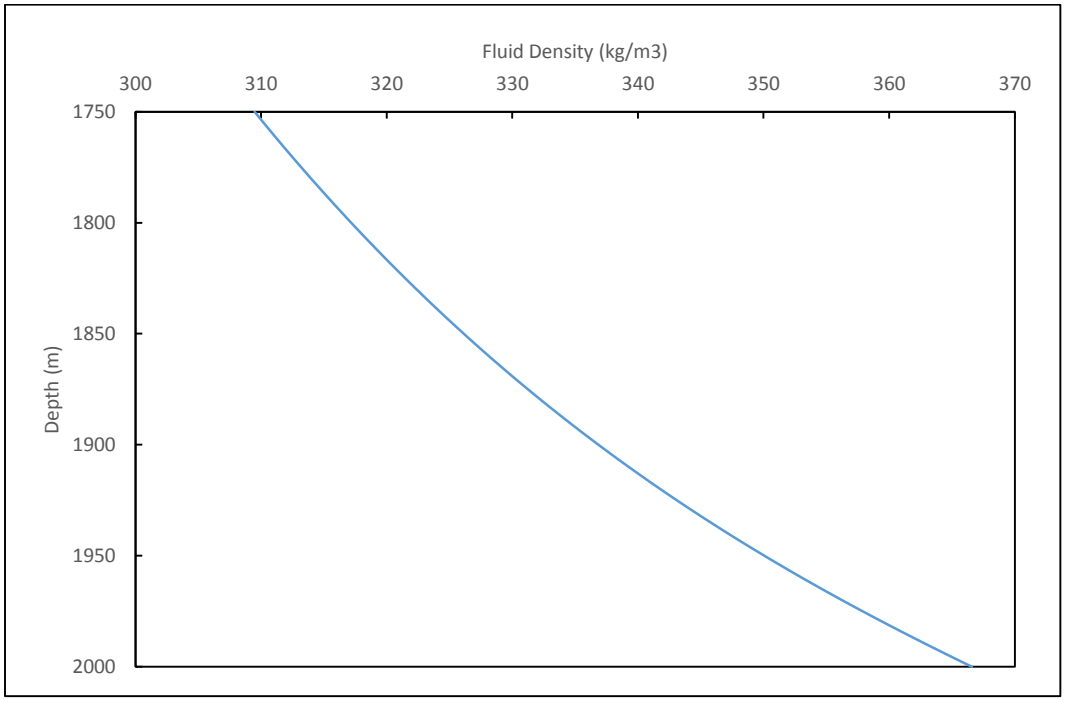

Figure 5.22. Case study 4, normal fluid density distribution

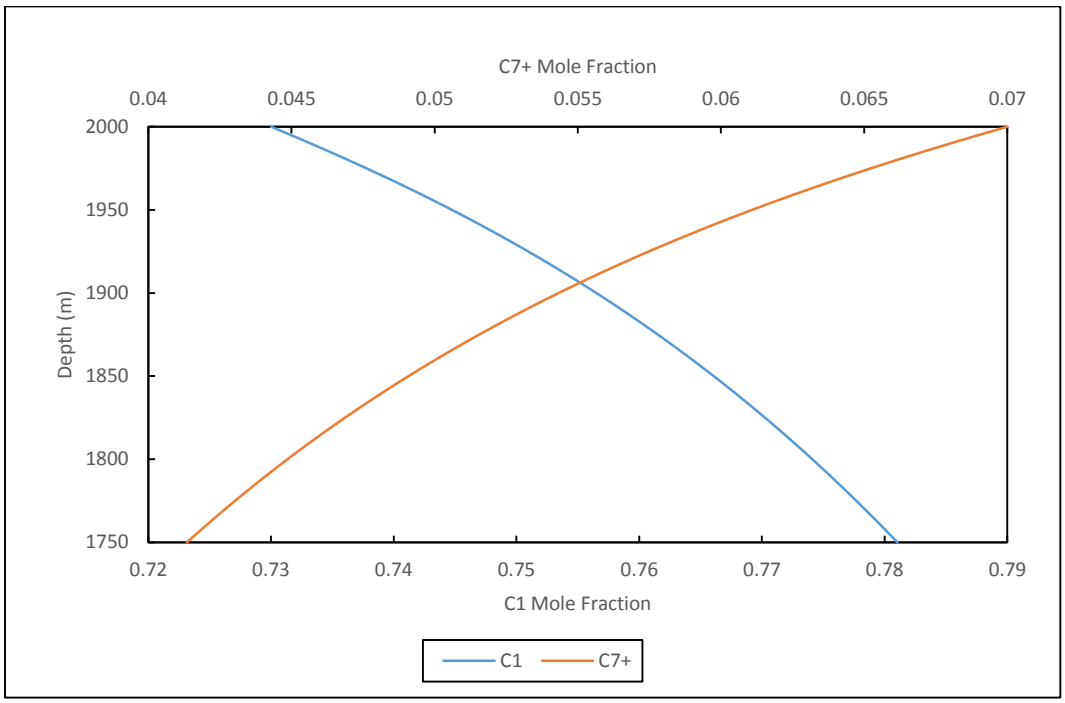

Figure 5.23. Case study 4, normal component distribution

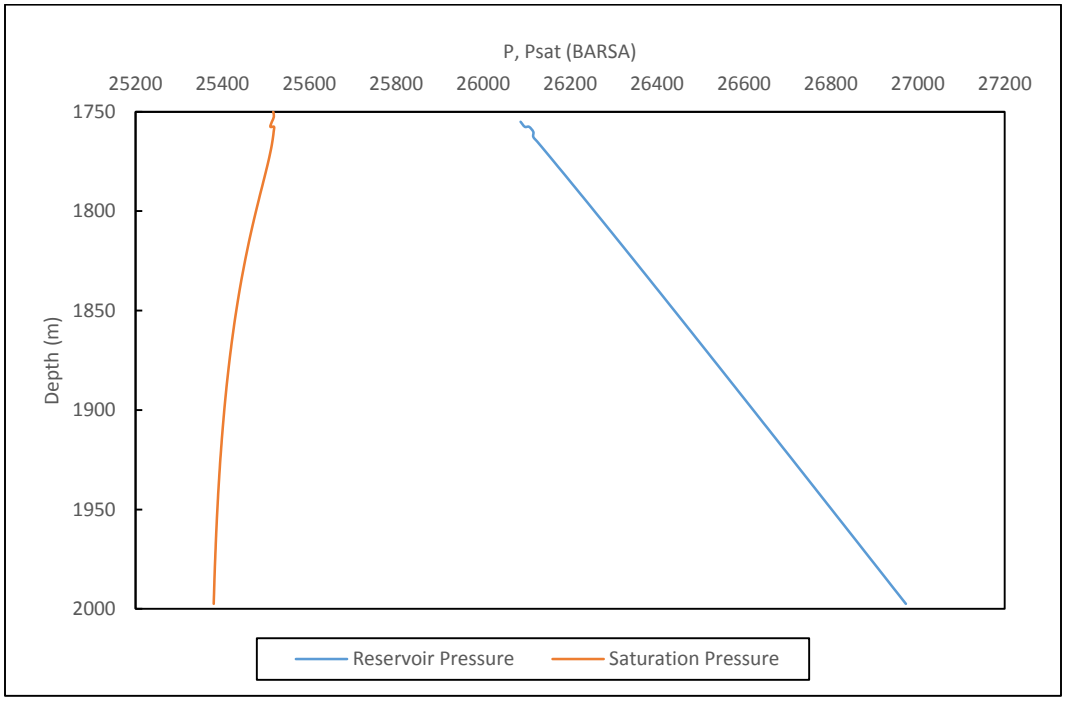

Figure 5.24. Case study 4, undersaturated system when gravitational and thermal effects are equal

The first case to investigate is an unusual case where there is an undersaturated GOC (Fig. 5.18) and a stable liquid column exits on the top of a stable gas column. The density ***decreases*** with depth in the reservoir (Fig. 5.19) due to the thermal diffusion effect (a temperature gradient of 0.025 K/m) being greater than that of the gravity. As seen in Fig. 5.20, the fluid is more concentrated in heavy component mole fraction and less in methane in shallower depths. This phenomenon is the opposite of what is usually observed in petroleum reservoirs while it has been reported to exist in some petroleum accumulations (Ghorayeb et al., 2000).

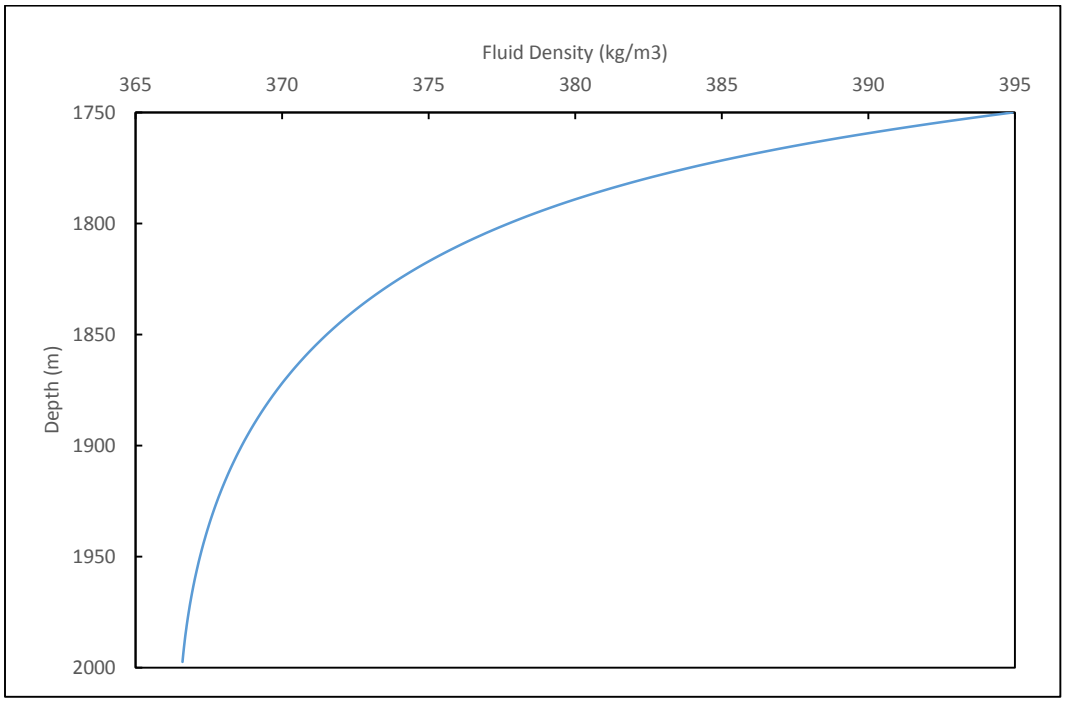

Figure 5.25. Case study 4, fluid density distribution when gravitational and thermal effects are equal

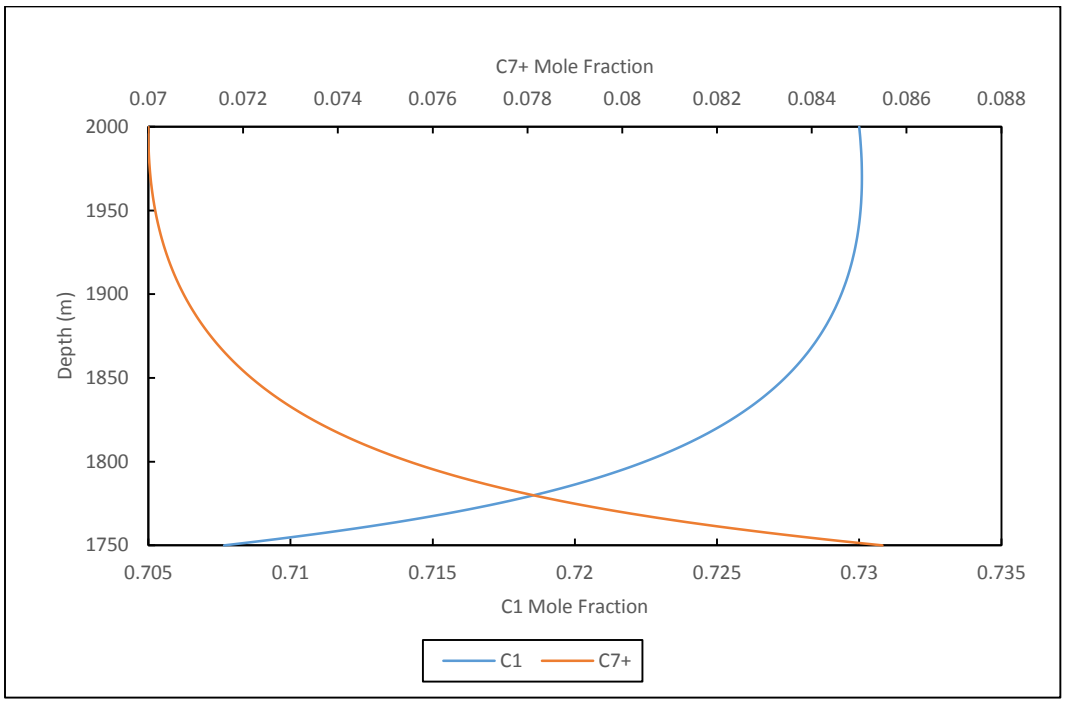

Figure 5.26. Case study 4, component distribution when gravitational and thermal effects are equal

Next, we investigate the condition when the gravitation and thermal diffusion effects are almost equal (but in opposite directions). We set the temperature gradient to 0.02 K/m. As seen in Figs. 5.24-5.26, at the beginning (the bottom of the reservoir is chosen as the reference point for CG calculations) the saturation pressure, density and composition are not changing while in the shallower points, the thermal effect is greater than the gravitational effect.

In this chapter we validated the nonisothermal CG numerical algorithm we proposed in chapter 4, we validated the plus fraction MW gradient model and showed how to model the sudden change of the plus fraction at the saturated GOC. The algorithm can predict the location of saturated and undersaturated GOC in the two-phase petroleum reservoir. We have shown the effect of EOS tuning in the CG calculation output. In a series of sensitivity analyses we showed how important the temperature gradient can be in modeling different fluid distribution schemes. The calculations

may not be valid when we have convection in the reservoir as we assumed the reservoir to be in stationary state to derive our model.

Conclusions

- We have simulated changes in composition of a petroleum fluid column with depth using EOS model, benefiting from thermodynamics of irreversible and reversible processes with the simplifying assumptions of stationary fluid systems with no convection.
- Our model predicts the location of GOC in saturated and undersaturated cases.
- Molecular weight and so all other properties of the plus fraction can change with depth, and gravity causes the fluid and the plus fraction to become heavier towards the bottom while a temperature gradient does the opposite.
- We have generalized the C7+ MW change with depth to the plus fraction‖ properties changes with depth in the nonisothermal reservoir. We showed the strategy to model the sharp change in the plus fraction MW at the saturated GOC.
- An isothermal model over-predicts the variation in composition of the reservoir fluid, so it is crucial to have correct information about a temperature gradient.
- Thermal diffusion usually acts in the opposite direction of the gravity in CG, and it can reduce or even totally eliminate the gravitational effect and cause a stable liquid to exist above gas in the reservoir.
- Near-critical fluids show higher and more nonlinear CG, and the reservoirs with this type of fluids can illustrate the case of an undersaturated GOC where the properties of liquid gradually change into gas without any sharp change in the density gradient. Therefore, dynamic fluid density logs cannot detect the location of the correct GOC.
- Changes in the BIP's and volume shifts can change the result of the CG calculations even when the fluid is tuned versus the same lab data but with different sets of tuning parameters. To obtain the correct reservoir EOS, it is highly recommended that a single EOS is tuned versus

lab data at different depths, and it will ensure that the CG model can correctly give the composition of all the samples at different depths when one sample at a single depth is chosen as the reference point to start the CG calculations.

References

Barrufet, M., and Jaramillo, J. (2004). Effects in the determination of oil reserves due to gravitational compositional gradients in near-critical reservoirs. *Journal of Canadian Petroleum Technology*, *43*(7).

Bearman, R. J., Kirkwood, J. G., and Fixman, M. (1958). Statistical-Mechanical Theory of Transport Processes. X. The Heat of Transport in Binary Liquid Solutions. Advances in Chemical Physics, Volume 1, 1-13

Bedrikovetsky, P. (1993). *Mathematical theory of oil and gas recovery: with applications to ex-USSR oil and gas fields* (Vol. 4). Springer.

Belery, P., and Da Silva, F. V. (1990). Gravity and thermal diffusion in hydrocarbon reservoirs. *Third Chalk Research Program*.

Chaback, J. J., and Lira-Galeana, C. (1992). Discussions of treatment of variations of composition with depth in gas-condensate reservoirs. *SPE reservoir engineering*, *7*(1), 157-158.

Computer Modeling Group. (2013). CMG suite of programs.

Creek, J. L., and Schrader, M. L. (1985, September). East Painter reservoir: an example of a compositional gradient from a gravitational field. In *SPE Annual Technical Conference and Exhibition*.

Danesh, A. (1998). *PVT and phase behaviour of petroleum reservoir fluids* (Vol. 47). Elsevier.

De Groot, S. R. (1951). *Thermodynamics of irreversible processes* (pp. 195-207). Amsterdam: North-Holland.

de Oliveira Padua, K. (1997, October). Non-Isothermal Gravitational Composition Variation in a Large Deep Water Field. In *SPE Annual Technical Conference and Exhibition*.

Dougherty Jr, E. L., and Drickamer, H. G. (1955). Thermal diffusion and molecular motion in liquids. *The Journal of Physical Chemistry*, *59*(5), 443-449.

Elshahawi, H., Hashem, M., Mullins, O., and Fujisawa, G. (2005, October). The missing link-identification of reservoir compartmentalization through downhole fluid analysis. In *SPE Annual Technical Conference and Exhibition*.

Elshahawi, H., Venkataramanan, L., McKinney, D., Flannery, M., Mullins, O., and Hashem, M. (2006, September). Combining Continuous Fluid Typing, Wireline Formation Tester, and Geochemical Measurements for an Improved Understanding of Reservoir Architecture. In *SPE Annual Technical Conference and Exhibition*.

Faissat, B., Knudsen, K., Stenby, E. H., and Montel, F. (1994). Fundamental statements about thermal diffusion for a multicomponent mixture in a porous medium. *Fluid phase equilibria*, *100*, 209-222.

Firoozabadi, A., Ghorayeb, K., and Shukla, K. (2000). Theoretical model of thermal diffusion factors in multicomponent mixtures. *AIChE Journal*, *46*(5), 892-900.

Ghorayeb, K., and Firoozabadi, A. (2000a). Numerical study of natural convection and diffusion in fractured porous media. *SPE Journal*, *5*(1), 12-20.

Ghorayeb, K., and Firoozabadi, A. (2000b). Modeling multicomponent diffusion and convection in porous media. *SPE Journal*, *5*(2), 158-171.

Ghorayeb, K., & Firoozabadi, A. (2000c). Molecular, pressure, and thermal diffusion in nonideal multicomponent mixtures. *AIChE journal*, *46*(5), 883-891.

Ghorayeb, K., Anraku, T., and Firoozabadi, A. (2000, April). Interpretation of the fluid distribution and GOR behavior in the Yufutsu fractured gas-condensate field. In *SPE Asia Pacific Conference on Integrated Modelling for Asset Management*.

Gibbs, J. W. (1961). The Scientific Papers of J. Willard Gibbs.

Gibson, A., Sorensen, H., Abdou, M., and Sener, I. (2006, November). New Methods for the Nonequilibrium Initialisation of Reservoir Models With Lateral and Vertical Variations in the Initial Fluid Composition. In *Abu Dhabi International Petroleum Exhibition and Conference*.

Haase, R. (1971). Borgmann H.W., Ducker KH., and Lee W.P. Thermodiffusion im Kritischen Verdampfunggsgebiet Binarer Systeme. *Z. Naturforsch. 26a*, *1224*.

Haase, R., and Haase, R. (1990). *Thermodynamics of irreversible processes* (p. 39). New York: Dover.

Hamoodi, A. N., Abed, A. F., and Jim, G. (1994, September). Modeling of a Large Gas-Capped Reservoir With Areal and Vertical Variation in Composition. In *SPE Annual Technical Conference and Exhibition*.

Hamoodi, A., Abed, A., and Firoozabadi, A. (2001). Compositional modelling of two-phase hydrocarbon reservoirs. *Journal of Canadian Petroleum Technology*, *40*(4).

Hirschberg, A. (1988). Role of asphaltenes in compositional grading of a reservoir's fluid column. *Journal of petroleum technology*, *40*(1), 89-94.

Hoier, L., and Whitson, C. H. (2001). Compositional Grading? Theory and Practice. *SPE Reservoir Evaluation and Engineering*, *4*(6), 525-535.

Hoier, L., and Whitson, C. H. (2001). Miscibility variation in compositionally grading reservoirs. *SPE Reservoir Evaluation and Engineering*, *4*(1), 36-43.

Hoier, L., Cheng, N., and Whitson, C. H. (2004, September). Miscible gas injection in undersaturated gas-oil systems. In *SPE Annual Technical Conference and Exhibition*.

Holt, T., Lindeberg, E., and Ratkje, S. K. (1983). The effect of gravity and temperature gradients on methane distribution in oil reservoirs. *unsolicited paper SPE*, *11761*.

Huang, W. W. (1985, September). Some Experiences With a Critical Reservoir Fluid. In *SPE Annual Technical Conference and Exhibition*.

Hussein, H., and Mahgoub, I. (2005, October). Methodology of Investigating the Compositional Gradient Within the Hydrocarbon Column. In *SPE Annual Technical Conference and Exhibition*.

Jacqmin, D. (1990). Interaction of natural convection and gravity segregation in oil/gas reservoirs. *SPE Reservoir Engineering*, *5*(2), 233-238.

Jessen, K., Gerritsen, M., and Mallison, B. (2008). High-resolution prediction of enhanced condensate recovery processes. *SPE Journal*, *13*(2), 257-266.

Kempers, L. J. T. M. (1989). A thermodynamic theory of the Soret effect in a multicomponent liquid. *The Journal of Chemical Physics*, *90*, 6541.

Lee, S. T. (1989, October). Capillary-gravity equilibria for hydrocarbon fluids in porous media. In *SPE Annual Technical Conference and Exhibition*.

Leverett, M. C. (1940). Capillary behavior in porous solids. *Trans. Am. Inst.*

Lira-Galeana, C., Firoozabadi, A., and Prausnitz, J. M. (1994). Computation of compositional grading in hydrocarbon reservoirs. Application of continuous thermodynamics. *Fluid Phase Equilibria*, *102*(2), 143-158.

Luo, S., and Barrufet, M. A. (2004). Compositional gradient: its role in near-critical reservoir development. *Journal of Petroleum Science and Engineering*, *45*(3), 193-201.

Manafi, H., Mansoori, G. A., and Ghotbi, S. (1999). Phase behavior prediction of petroleum fluids with minimum characterization data. *Journal of Petroleum Science and Engineering*, *22*(1), 67-93.

Metcalfe, R. S., Vogel, J. L., and Morris, R. W. (1988). Compositional gradients in the Anschutz Ranch east field. *SPE reservoir engineering*, *3*(3), 1025-1032.

Montel, F., and Gouel, P. L. (1985, September). Prediction of compositional grading in a reservoir fluid column. In *SPE Annual Technical Conference and Exhibition*.

Montel, F., Bickert, J., Hy-Billiot, J., and Royer, M. (2003, August). Pressure and compositional gradients in reservoirs. In *Nigeria Annual International Conference and Exhibition*.

Muskat, M. (1930). Distribution of non-reacting fluids in the gravitational field. *Physical Review*, *35*(11), 1384.

Nasrabadi, H. Compositional Variation in Two-Phase Hydrocarbon Reservoirs from Diffusion and Natural Convection, *PhD Dissertation*, Imperial College, London, United Kingdom (2006).

Nasrabadi, H., Firoozabadi, A., Esposito, R., and Vieira, A. (2008, June). Interpretation of an unusual bubblepoint pressure variation in an offshore field. In *Europec/EAGE Conference and Exhibition*.

Nia, N. B., and Movagharnejad, K. (2007). Prediction of heptane plus fraction molecular weight variation in hydrocarbon reservoirs. *Fluid Phase Equilibria*, *262*(1), 174-179.

Nikpoor, M. H., & Chen, Z. (2013). New Methodology for the Modeling of Compositional Grading within the Gas-Oil Transition Zone in Petroleum Reservoirs. *Energy Sources, Part A: Recovery, Utilization, and Environmental Effects*, *35*(5), 438-444.

Nikpoor, M. H., Kharrat, R., & Chen, Z. (2011). Modeling of compositional grading and plus fraction properties changes with depth in petroleum reservoirs. *Petroleum Science and Technology*, *29*(9), 914-923.

Onsager, L. (1931a). Reciprocal relations in irreversible processes. I. *Physical Review*, *37*(4), 405.

Onsager, L. (1931b). Reciprocal relations in irreversible processes. II. *Physical Review*, *38*(12), 2265.

Pedersen, K. S., Blilie, A. L., & Meisingset, K. K. (1992). PVT calculations on petroleum reservoir fluids using measured and estimated compositional data for the plus fraction. *Industrial & engineering chemistry research*, *31*(5), 1378-1384.

Pedersen, K. S., and Lindeloff, N. (2003, October). Simulations of compositional gradients in hydrocarbon reservoirs under the influence of a temperature gradient. In *SPE Annual Technical Conference and Exhibition*.

Peng, D. Y., and Robinson, D. B. (1976). A new two-constant equation of state. *Industrial and Engineering Chemistry Fundamentals*, *15*(1), 59-64.

Ratulowski, J., Fuex, A. N., Westrich, J. T., and Sieler, J. J. (2003). Theoretical and experimental investigation of isothermal compositional grading. *SPE Reservoir Evaluation and Engineering*, *6*(3), 168-175.

Riemens, W. G., and Schulte, A. M. (1988). Birba field PVT variations along the hydrocarbon column and confirmatory field tests. *Journal of petroleum technology*, *40*(1), 83-88.

Sage, B. H., and Lacey, W. N. (1939). Gravitational concentration gradients in static columns of hydrocarbon fluids. *Trans. AIME*, *132*, 120-131.

Salehirad, Y. (2005, October). Effect of Compositional Grading on Reservoir Fluid Characterization: Case Study. In *SPE Annual Technical Conference and Exhibition*.

Schlumberger. (2005). ECLIPSE suite of programs.

Schou Pedersen, K., and Hjermstad, H. (2006, November). Modeling of Large Hydrocarbon Compositional Gradient. In *Abu Dhabi International Petroleum Exhibition and Conference*.

Schulte, A. M. (1980, September). Compositional variations within a hydrocarbon column due to gravity. In *SPE annual technical conference and exhibition*.

Sigmund, P. M., Dranchuk, P. M., Morrow, N. R., and Purvis, R. A. (1973). Retrograde condensation in porous media. *Old SPE Journal*, *13*(2), 93-104.

Smalley, P. C., and England, W. A. (1992). SPE 25005 Assessing Reservoir Compartmentalization During Field Appraisal: How Geochemistry Can Help. In *European Petroleum Conference* (pp. 423-423).

Sognesand, S. (1997). Reservoir management of the Oseberg Field during eight years' production. *Offshore Europe*.

Syahrial, E. (1999, April). Impact of composition variation with depth on volatile oil. In *SPE Asia Pacific Oil and Gas Conference and Exhibition*.

Temeng, K. O., Al-Sadeg, M. J., and Al-Mulhim, W. A. (1998, September). Compositional grading in the Ghawar Khuff reservoirs. In *SPE Annual Technical Conference and Exhibition*.

Trebin, F. A. and Zadora, G. I. (1968). Experimental Study of the Influence of a Porous Medium on the Phase Transformations of Gas-Condensate Systems. *Neft' i Gas* (8).

Tyrrell, H. J. V. (1961). *Diffusion and heat flow in liquids* (p. 44). London: Butterworths.

Wheaton, R. J. (1991). Treatment of Variations of Composition With Depth in Gas-Condensate Reservoirs (includes associated papers 23549 and 24109). *SPE Reservoir Engineering*, *6*(2), 239-244.

Whitson, C. H., and Belery, P. (1994, August). Compositional gradients in petroleum reservoirs. In *University of Tulsa Centennial Petroleum Engineering Symposium*.

Appendix A: Cubic EOS

A.1 Introduction

Cubic EOS's are simple equations relating pressure, volume, and temperature (PVT). They accurately describe the volumetric and phase behavior of pure compounds and mixtures, requiring only critical properties and acentric factor of each component. The same equation is used to calculate the properties of all phases, thereby ensuring consistency in reservoir processes that approach critical conditions (e.g., miscible-gas injection and depletion of volatile-oil/gas-condensate reservoirs). Volumetric behavior is calculated by solving a simple cubic equation, usually expressed in terms of $Z=Pv/RT$:

$$Z^3 + A_2 Z^2 + A_1 Z + A_0 = 0 \qquad \text{(A.1)}$$

where constants A_0, A_1, and A_2 are functions of pressure, temperature, and phase composition. Phase equilibria are calculated with an EOS by satisfying the condition of chemical equilibrium. For a two-phase system, the chemical potential of each component in the liquid phase $\mu_i(x)$ must equal the chemical potential of each component in the vapor phase $\mu_i(y)$, $\mu_i(x) = \mu_i(y)$. Chemical potential is usually expressed in terms of fugacity, f_i, where $\mu_i = RT \ln f_i + \lambda_i(T)$ and $\lambda_i(T)$ are constant terms that drop out in most problems. It is readily shown that the condition $\mu_i(x) = \mu_i(y)$ is satisfied by the equal-fugacity constraint, $f_i(x) = f_i(y)$, where fugacity is given by:

$$\ln \phi_i = \ln \frac{f_i}{y_i P} = \frac{1}{RT} \int_V^\infty \left(\frac{\partial P}{\partial n_i} - \frac{RT}{V} \right) dV - \ln Z \qquad \text{(A.2)}$$

Other thermodynamic properties, such as Helmholz energy, enthalpy, and entropy, can be readily defined in terms of the fugacity coefficient. Michelsen (1986) gives a particularly compact and

useful discussion of the relation between thermodynamic properties aimed at making efficient EOS calculations.

A component material balance is also required to solve VLE problems: $z_i = F^V y_i + \left(1 - F^V\right) x_i$, where F^V is the mole fraction of the system in the vapor phase equal to $n^V / \left(n^V + n^L\right)$.

Solving phase equilibria with an EOS is a trial-and-error procedure, requiring considerable computations. With today's computers, however, the task is fast and reliable. The accuracy of EOS predictions has also improved considerably during the past 15 years, during which emphasis has been on improved liquid volumetric predictions and treating the heptane-plus fraction.

This appendix provides the equations and algorithms necessary for calculating phase and volumetric behavior of reservoir fluids with a cubic EOS.

A.2 Cubic EOS and Fugacity Calculation

A cubic EOS takes the general form:

$$P = \frac{RT}{v - b} - \frac{a}{\left(v + \delta_1 b\right)\left(v + \delta_2 b\right)} \tag{A.3}$$

where δ_1 and δ_2 are constants for the chosen EOS; when $\delta_1 = 1 - \sqrt{2}$ and $\delta_2 = 1 + \sqrt{2}$ it becomes the Peng-Robinson (PR) EOS and when $\delta_1 = 1$ and $\delta_2 = 0$, it becomes the Soave-Redlich-Kwong (SRK) EOS.

For pure components, the parameters *a* and *b* are expressed in terms of the critical properties and the acentric factor:

$$a = a_c \alpha \tag{A.4}$$

$$a_c = \Omega_a \left(RT_c\right)^2 / P_c \tag{A.5}$$

$$\alpha = \left(1 + m\left[1 - \sqrt{T/T_c}\right]\right)^2 \tag{A.6}$$

$$b = \Omega_b RT_c / P_c \tag{A.7}$$

Selection of the parameters Ω_a and Ω_b depends on the chosen EOS; for the PR EOS they are 0.45724 and 0.07780, respectively, while for the SOR EOS the values are 0.42747 and 0.08664. Factor *m* is conventionally calculated as a polynomial function of the acentric factor.

Usually the phase behavior equations turn into simpler forms by introducing dimensionless *A* and *B*:

$$\begin{aligned} A &= aP/(RT)^2 \\ B &= bP/RT \end{aligned} \tag{A.8}$$

Then the coefficients in Eq. (A.1) can be calculated as:

$$A_2 = B(f_1 - 1) - 1 \tag{A.9}$$

$$A_1 = A - f_1 B + (f_2 - f_1) B^2 \tag{A.10}$$

$$A_0 = -f_2 (B^3 + B^2) - AB \tag{A.11}$$

where

$$\begin{aligned} f_1 &= \delta_1 + \delta_2 \\ f_2 &= \delta_1 \delta_2 \end{aligned} \tag{A.12}$$

For mixtures, the parameters *a* and *b* are defined using the following mixing rules:

$$a = \sum_i x_i t_i \tag{A.13}$$

$$t_i = \sum_j x_j (1 - K_{ij}) \sqrt{a_{ij}} \tag{A.14}$$

$$a_{ij} = a_i a_j \tag{A.15}$$

$$b = \sum_i x_i b_i \tag{A.16}$$

where K_{ij} is the binary interaction parameter.

Solving the integral in Eq. (A.2) results in:

$$\ln \phi_i = \frac{b_i}{b}(Z-1) - \ln(Z-B) - \frac{A}{(\delta_2 - \delta_1)B}\left(\frac{2t_i}{a} - \frac{b_i}{b}\right)\ln\frac{Z+\delta_2 B}{Z+\delta_1 B} \tag{A.17}$$

A.3 Volume Shift Technique

The volume translation technique of Peneloux et al (1982) is used to improve the density prediction capability of the SRK and PR EOS's. A volume translation modifies the molar volume of the system v predicted by the EOS as follows:

$$v^c = v - c \tag{A.18}$$

$$c = \sum x_i c_i \tag{A.19}$$

$$v_i^c = v_i - c_i \tag{A.20}$$

$$c_i = S_i b_i \tag{A.21}$$

In the above equations, v^c is the corrected volume, v is the volume calculated by EOS, c is the volume correction, v_i is the partial volume, c_i is the partial volume correction and S_i is called the dimensionless volume translation parameter which is conventionally calculated using empirical correlations. Consider the equation for a fugacity coefficient:

$$\ln \phi_i = \int_0^P (v_i/RT - 1/P)dP \tag{A.22}$$

Now, considering the Eq. (A.20) and the assumption that S_i is pressure-independent we can conclude:

$$\ln \phi_i^c = \ln \phi_i - c_i P/RT \tag{A.23}$$

and as a result, the fugacity changes by:

$$f_i^c = f_i \exp\left(-c_i P/RT\right) \tag{A.24}$$

The same volume correction is applied for the gas and the liquid phases in VLE calculations and considering:

$$K_i = y_i/x_i = \phi_i^L/\phi_i^V \tag{A.25}$$

then the K values remain the same as before and volume translation has no effect on the phase equilibrium calculations. In the CG calculations:

$$RTd_T \ln f_k = M_k g dh - \frac{Q_k^{net}}{T} dT \tag{3.58}$$

we can conclude that:

$$RT\left(\ln f_i^{c,h}\left(P^h,T\right) - \ln f_i^{c,h^0}\left(P^{h^0},T\right)\right) = M_k g dh - \frac{Q_k^{net}}{T} dT \tag{A.26}$$

and from Eq. (A.23) we can reach the following equation:

$$RT\left(\ln f_i^{h}\left(P^h,T\right) - \ln f_i^{h^0}\left(P^{h^0},T\right)\right) = M_k g dh - \frac{Q_k^{net}}{T} dT + \frac{c_i\left[P^h - P^{h^0}\right]}{RT} \tag{A.26}$$

Accordingly, the volume correction changes the CG calculations. Furthermore, in the calculation of NHT, we have:

$$\Delta\overline{U}_i = \overline{U}_i^R = \overline{H}_i^R - P.\bar{v}_i^R \tag{4.19}$$

where:

$$\overline{H}_i^R = -RT^2 \frac{\partial \ln \varphi_i}{\partial T} \tag{4.20}$$

$$\bar{v}_i^R = \bar{v}_i - RT/P \tag{4.21}$$

Then the NHT is also affected by the volume correction.

For a more complete discussion about phase behavior and EOS calculation refer to Danesh (1998) and the Winprop software manual (Computer Modeling Group Ltd., 2013).

References for Appendix A

Computer Modeling Group. (2013). CMG suite of programs.

Danesh, A. (1998). *PVT and phase behaviour of petroleum reservoir fluids* (Vol. 47). Elsevier.

Michelsen, M. L., & Mollerup, J. (1986). Partial derivatives of thermodynamic properties. *AIChE journal*, *32*(8), 1389-1392.

Péneloux, A., Rauzy, E., & Fréze, R. (1982). A consistent correction for Redlich-Kwong-Soave volumes. *Fluid Phase Equilibria*, *8*(1), 7-23.

Appendix B: Fundamentals of Phase Equilibrium Calculations

B.1 Introduction

In this appendix, we state the condition for phase equilibrium in the mathematical form and bring the fundamental equations the reader needs in order to completely understand the materials provided in this thesis. We start with the fundamental criteria for stability and phase equilibrium and then introduce the equations needed to be solved for phase equilibrium calculations. We primarily focus on VLE as other kinds of phase equilibria are out of the scope of this work.

B.2 Criteria for Equilibrium

A system of overall composition n_i is stable if its Gibbs energy, G, reaches the ultimate minimum at the specified pressure, P, and temperature, T, (Danesh, 1998) which implies that:

$$(\partial G)_{P,T} = 0 \qquad \text{(B.1)}$$

and

$$(\partial^2 G)_{P,T} > 0 \qquad \text{(B.2)}$$

The minimum Gibbs energy, as the general criterion of equilibrium, is often used to derive working expressions. At equilibrium, the system energy is at its lowest value amongst all possible conditions, including all possible minima occurring in the calculated Gibbs energy function. Hence the equilibrium should be determined by searching for the global minimum value of the Gibbs energy.

Assuming the final system to have π phases in equilibrium and re-writing the first equation in terms of chemical potentials, μ_i, and n_i:

$$\left(dG\right)_{P,T} = \sum_{j=1}^{\pi}\left(\sum_{i=1}^{n}\mu_i dn_i\right)_j = 0 \qquad \text{(B.3)}$$

Restricting the overall composition to be n_i:

$$dn_i = \sum_{j=1}^{\pi} \left(dn_i \right)_j = 0 \ , \ i = 1, 2, ...n \tag{B.4}$$

Considering Eqs. (B.3) and (B.4) we obtain:

$$\mu_i^{(1)} = \mu_i^{(2)} = ... = \mu_i^{(\pi)} \tag{B.5}$$

The above general requirement, that is, the equality of chemical potential of each component throughout all the co-existing phases at equilibrium, becomes a practical engineering tool if the chemical potential can be related to measurable quantities. This is achieved by expressing the chemical potential in terms of auxiliary thermodynamic functions, such as fugacity or activity.

B.3 Equilibrium Condition for Systems Involving Vapor and Liquid

The relationship between chemical potential and fugacity, f_i is stated as:

$$\mu_i = \mu_i^0 = RT \ln\left(f_i / f_i^0 \right) \tag{B.6}$$

where μ_i^0 and f_i^0 are the chemical potential and fugacity of the component i, respectively, at a reference state.

Writing Eq. (B.6) for the component i in both phases of a heterogeneous system, with the vapor and liquid reference states at the same temperature, the equality of the chemical potential at equilibrium given by Eq. (B.5) leads to:

$$f_i^V = f_i^L \tag{B.7}$$

That is, the fugacity of each component should be equal throughout all the phases in a heterogeneous system at equilibrium.

In applications, fugacity is related to the fugacity coefficient, φ_i, by:

$$\begin{aligned} f_i^L &= x_i P \varphi_i^L \\ f_i^V &= y_i P \varphi_i^V \end{aligned} \tag{B.8}$$

where x_i and y_i show the composition of the liquid and vapor phases, respectively. Now, we use Eqs. (B.7) and (B.8) and introduce the concept of an equilibrium ratio K_i as:

$$K_i = y_i / x_i = \varphi_i^L / \varphi_i^V \tag{B.9}$$

In a phase split and stability analysis, it is usually the K_i which is used instead of compositions as the primary variables. Apparently, K_i can be calculated by the EOS if the vapor and liquid phase compositions are known.

B.4 Vapor-Liquid Equilibrium Calculations

Let one mole of a mixture be flashed at pressure P and temperature T into F^L moles of liquid and F^V moles of vapor. The total material balance equations for the system are:

$$F^L + F^V = 1 \tag{B.10}$$

$$\sum_{i=1}^{n} x_i = \sum_{i=1}^{n} y_i = 1 \tag{B.11}$$

Considering the component material balance:

$$z_i = F^L x_i + F^V y_i \tag{B.12}$$

after some mathematical manipulation, we reach the following equations:

$$\sum_{i=1}^{n} x_i = \sum_{i=1}^{n} \frac{z_i}{1+\left(K_i - 1\right)F^V} = 1 \tag{B.13}$$

$$\sum_{i=1}^{n} y_i = \sum_{i=1}^{n} \frac{Kz_i}{1+\left(K_i - 1\right)F^V} = 1 \tag{B.14}$$

Alternatively, combining the two equations leads to the Rachford-Rice (Rachford and Rice, 1952) equation:

$$Q\left(F^V\right) = \sum_{i=1}^{n} \left(y_i - x_i\right) = \sum_{i=1}^{n} \frac{z_i\left(K_i - 1\right)}{1+\left(K_i - 1\right)F^V} = 0 \tag{B.15}$$

The above equation yields a physically correct root for F^V between 0 and 1, provided that:

$$S^V = \sum_{i=1}^{n} K_i z_i > 0 \;\; and \;\; S^L = \sum_{i=1}^{n} z_i / K_i > 0 \tag{B.16}$$

The mixture is at its bubble point when F^V approaches zero. Hence Eq. (B.15) reduces to:

$$S^V = \sum_{i=1}^{n} K_i z_i = 1 \;\; and \;\; y_i = K_i x_i = K_i z_i \tag{B.17}$$

At any temperature the bubble point pressure can be determined as the pressure at which the K values satisfy Eq. (B.17). The bubble point is most sensitive to the mixture light components, which exhibit large K values.

At the dew point, F^V approaches 1. Hence Eq. (B.15) reduces to:

$$S^L = \sum_{i=1}^{n} z_i / K_i = 1 \;\; and \;\; x_i = y_i / K_i = z_i / K_i \tag{B.18}$$

The dew point pressure is that at which the K-values satisfy Eq. (B.17). The dew point is most sensitive to the mixture heavy components, which exhibit small K-values.

The above identification is valid if reasonably accurate K values are used. A more rigorous approach to identify the state of a mixture is given in Section B.5 using the Gibbs energy minimization method.

At low and moderate pressures, where the dependence of an equilibrium ratio on phase composition can be neglected, flash calculations are relatively simple, as the K values are known. In general, the K-values vary with composition, and hence the solution is reached by iteration.

The calculation can begin by initializing K values in Eq. (B.15) estimated from the Wilson correlation (Wilson, 1969):

$$K_i = \left(P_{ci}/P\right) \exp\left[5.37\left(1+\omega_i\right)\left(1-T_{ci}/T\right)\right] \tag{B.19}$$

The solution of Eq. (B.15) yields the compositions of the two phases using Eqs. (B.13) and (B.14). The calculated compositions are then used to re-evaluate the K values, using the EOS and Eq. (B.9), to be substituted in Eq. (B.15) for the next round of iteration. The iterative calculations are complete when values of checked functions are all smaller than certain pre-set tolerances.

B.5 Stability Analysis

At a given temperature and pressure, the number of phases may not always be known in advance. The Gibbs phase rule does not impose any practical limitation on the number of possible phases, in real reservoir fluids, as they are composed of many components.

Traditionally, this problem has been solved either by conducting a two-phase flash or by making a saturation-pressure calculation; both methods are expensive and not entirely reliable.

The rigorous method of determining the equilibrium at a given pressure and temperature is to find the conditions at which the Gibbs energy of the system is at its global minimum for all possible combinations of phases and component distribution, which was expressed mathematically in Eqs. (B.1) and (B.2).

As it is impractical to investigate all the possible combinations of phases and distribution (satisfying the overall and component material balance), Michelsen (1982) proposed introducing an infinitesimal amount of new test phases and investigating if it can lead to finding a local minimum in the Gibbs energy surface (i.e., equality of the fugacities). He showed how the Gibbs tangent-plane criterion could be used to establish the thermodynamic stability of a phase (i.e., whether a given composition has a lower energy remaining as a single phase (stable) or whether the mixture Gibbs energy will decrease by splitting the mixture into two or more phases (unstable)). The algorithm starts with guessing a new phase composition (or a set of K values defining the new phase composition with respect to the original phase composition) with an

infinitesimal amount and then updating the composition of this new phase in the hope of finding a non-trivial solution similar to what was discussed in case of the VLE flash calculations in the previous section.

References for Appendix B

Danesh, A. (1998). *PVT and phase behaviour of petroleum reservoir fluids* (Vol. 47). Elsevier.

Michelsen, M. L. (1982). The isothermal flash problem. Part I. Stability. *Fluid Phase Equilibria*, *9*(1), 1-19.

Rachford Jr, H. H., & Rice, J. D. (1952). Procedure for use of electronic digital computers in calculating flash vaporization hydrocarbon equilibrium. *Journal of Petroleum Technology*, *4*(10).

Wilson, G. M. (1969, May). A modified Redlich-Kwong equation of state, application to general physical data calculations. In *65th National AIChE Meeting, Cleveland, OH*.